Available online at www.sciencedirect.com
ScienceDirect
Geomorphology 100 (2008) 527–548
GEOMORPHOLOGY
www.elsevier.com/locate/geomorph

Relationships between mesoscale morphological units, stream hydraulics and Chinook salmon (*Oncorhynchus tshawytscha*) spawning habitat on the Lower Yuba River, California

Hamish J. Moir *, Gregory B. Pasternack

Department of Land, Air, and Water Resources, University of California, One Shields Avenue, Davis, CA 95616-8626, USA

Received 8 October 2006; received in revised form 31 January 2008; accepted 1 February 2008
Available online 14 February 2008

Abstract

An expert-based approach was used to identify 10 morphological unit types within a reach of the gravel bed, regulated Yuba River, California, that is heavily utilized by spawning Chinook salmon (*Oncorhynchus tshawytscha*). Analysis of these units was carried out using two-dimensional hydrodynamic modeling, field-based geomorphic assessment, and detailed spawning surveying. Differently classified morphological units tended to exhibit discrete hydraulic signatures. In most cases, the Froude number adequately differentiated morphological units, but joint depth–velocity distributions proved the most effective hydraulic classification approach. Spawning activity was statistically differentiated at the mesoscale of the morphological unit. Salmon preferred lateral bar, riffle, and riffle entrance units. These units had moderately high velocity (unit median >0.45 m s^{-1}) and low depth (unit median <0.6 m), but each exhibited a unique joint depth–velocity distribution. A large proportion of redds (79%) were associated with conditions of convective flow acceleration at riffle and riffle entrance locations. In addition to reflecting microhabitat requirements of fish, it was proposed that the hydraulic segregation of preferred from avoided or tolerated morphological units was linked to the mutual association of specific hydraulic conditions with suitable caliber sediment that promotes the provision and maintenance of spawning habitat.

Keywords: Chinook salmon; Spawning; Morphological units; Hydraulics; Two-dimensional modeling; Fluvial geomorphology

1. Introduction

When viewed in terms of their role supporting ecological functions, fluvial processes may be differentiated by spatial scale relative to channel width (w) into those occurring at micro (0.01–1.0 w), meso (1.0–10 w), and larger spatial scales >10 w commonly referred to as reaches and/or segments depending on the classification system (e.g., Grant and Swanson, 1995; Montgomery and Buffington, 1997; Thompson et al., 2001). The term "microhabitat" is defined as the localized depth, velocity, temperature, and substrate at a point in a river without regard to the surrounding conditions. It is often possible to empirically relate ecological function to microhabitat variables (Bovee, 1986), but doing so provides a limited understanding of how and why fluvial–ecological linkages are spatially related. The term "mesohabitat" is defined as the interdependent set of the same physical variables over a discernible landform known as a morphological unit (e.g., scour pool, riffle, and lateral bar). There is a general lack of studies that nest the microscale requirements of instream species within the mesoscale context of an assemblage of morphological units. Consequently, in this study it is hypothesized that by linking the mesoscale of morphological units to microhabitat characteristics, it would be possible to explain fluvial–ecological linkages better.

Previous studies have provided justification why morphological units should be able to explain fluvial–ecological relations. First, they are considered to be the "fundamental building blocks of rivers systems" (Brierly and Fryirs, 2000). Also at the mesoscale, the concept of physical biotopes has been proposed as a framework for classifying streams based on their physical characteristics that is typically linked to instream habitats

* Corresponding author. The Macaulay Institute, Craigiebuckler, Aberdeen, AB15 8QH, UK. Fax: +44 1224 311556.
E-mail addresses: h.moir@macaulay.ac.uk (H.J. Moir), gpast@ucdavis.edu (G.B. Pasternack).

0169-555X/$ - see front matter © 2008 Elsevier B.V. All rights reserved.
doi:10.1016/j.geomorph.2008.02.001

(Padmore et al., 1998). Newson and Newson (2000) stated that a "biotope approach represents an important linking scale between the detail of microscale habitat hydraulics and the need for network-scale appraisals for management of channels and flows." Second, some studies have found that mesohabitat is a good predictor of fish utilization patterns (Geist and Dauble, 1998; Hanrahan, 2007). Finally, the type and distribution of morphological units have been found to be sensitive to landuse within the watershed (Beechie et al., 2003). In terms of practicality, the mesoscale provides a manageable resolution of analysis that balances scientific detail with the potential for catchment-scale application (Padmore et al., 1998); the study of the form, function and distribution of morphological units is therefore useful both in terms of scaling-up to watershed scale estimates of habitat capacity and for assessing how this might be impacted by human activity (Reeves et al., 1989; Beechie et al., 2001).

Although more general mesoscale research of habitat-types has been undertaken (Jowett, 1993; Orth, 1995), this has rarely involved specific studies of salmonid spawning habitat in anything but small streams (e.g., Moir et al., 2006). In many river systems spawning habitat has been identified as a key limiting factor controlling salmonid population sizes. Because salmonids spawn in gravel beds with heterogeneous features (Wheaton et al., 2004b), habitat availability and distribution depend on the physical character of stream channels at the mesoscale (Moyle, 1994; Montgomery et al., 1999; Brown, 2000). Yet most salmonid spawning studies have characterized microhabitats (e.g., Burner, 1951; Beland et al., 1982; Moir et al., 2002) or made more general and qualitative links to geomorphic form and process (e.g. Shirvell, 1989; Magee et al., 1996; Montgomery et al., 1996; Payne and Lapointe, 1997; Geist and Dauble, 1998; Knapp and Preisler, 1999; Dauble and Geist, 2000; Fukushima, 2001; Moir et al., 2002). Montgomery et al. (1999) and Moir et al. (2004) linked salmonid spawning habitat to a qualitative characterization of channel morphology, although both studies were explicitly reach scale, too coarse to resolve unit-specific geomorphic–biotic relationships. Few have explicitly examined the mesoscale, made quantitative physical–biotic linkages or assessed across spatial scales (e.g., characterized microscale hydraulic patterns nested within mesoscale units). Furthermore, the majority of studies examining salmonid spawning habitat have been conducted in relatively small streams where biological assessment (e.g., redd counts and spawning observation) and physical measurements (hydraulics and sediments) are less logistically demanding.

Moir et al. (2006) adopted a mesoscale approach to study the relationships between channel morphology, hydraulics, and Atlantic salmon spawning activity over a range of discharges at six study sites in an upland Scottish stream. Statistically significant differences in discharge–hydraulic relationships between the contrasting morphological unit types were identified. However, only morphological units utilized for spawning were studied; no comparison was made between spawning and non-spawning units. Also, instream hydraulics were sampled at a relatively low resolution (average of 0.081 points·m^{-2}) that may not have been sufficient to identify complex hydraulic patterns that are potentially important to habitat selection by spawning salmonids. Indeed, due to the inherent difficulties involved in representatively characterizing such phenomena, few studies have considered nonuniform hydraulic patterns (e.g., convergence, divergence, vorticity) at the mesoscale, factors that are known to be important geomorphic (Pasternack et al., 2006; MacWilliams et al., 2006; Brown and Pasternack, in press) and biological (Crowder and Diplas, 2002, 2006; Elkins et al., 2007) agents.

This study aimed to identify specific mesoscale morphological units associated with Chinook salmon (*Oncorhynchus tshawytscha*) spawning habitat in a large gravel-bed river and link them explicitly to microscale hydraulic patterns, sedimentary characteristics, and the geomorphic processes that control their character and distribution. Specifically, the objectives of the study were to (i) identify and map the distribution of morphological units, (ii) report their microhabitat characteristics, (iii) relate patterns of Chinook salmon spawning activity to the spatial distribution of morphological units and their hydraulic characteristics, and, (iv) describe the association between Chinook salmon spawning habitat, nonuniform hydraulics, and geomorphic processes.

The study was carried out at a site on the mainstem Yuba River, California adopting a combination of high-resolution topographic surveys, two-dimensional hydrodynamic modeling, and field-based biological and geomorphic analyses. Compared to other methods of assessment (e.g., one-dimensional models, cross-sectional assessments), the application of a two-dimensional hydrodynamic model allowed a closer representation of the resolution at which salmon select spawning sites and a better characterization of the broader scale flow patterns (e.g., convective acceleration, turbulent eddies, shear zones) that may be important in providing habitat. Understanding the geomorphic processes that control the ecological functioning and evolution of salmonid habitats is essential to determine the likely ecological effects of changes to the sediment and water budgets of a river system (through river management, landuse or climate change) and to guide science-based sustainable habitat rehabilitation.

2. Study area

The Yuba River is a tributary of the Sacramento River in the northern central valley of California (Fig. 1). It drains 3480 km^2 from the crest of the Sierra Nevada (highest elevation is Mount Lola at 2774 m amsl) to the confluence of the Feather River near Marysville and Yuba City (~10 m amsl). Flowing in a southwesterly direction, it grades from mountainous and forested in the headwaters to foothill terrain and then to a wide-open valley. Annual precipitation ranges from >1500 mm at the Sierra Nevada crest to ~500 mm at Marysville, ~85% of which falls between November and April (Curtis et al., 2005). In the upper regions of the catchment, much of this accumulates as snow pack that contributes significantly to spring runoff April–July.

The Yuba basin has been highly manipulated for hydropower, water supply, flood regulation, gold mining, and sediment control (James, 2005). Although two small dams exist on the South and

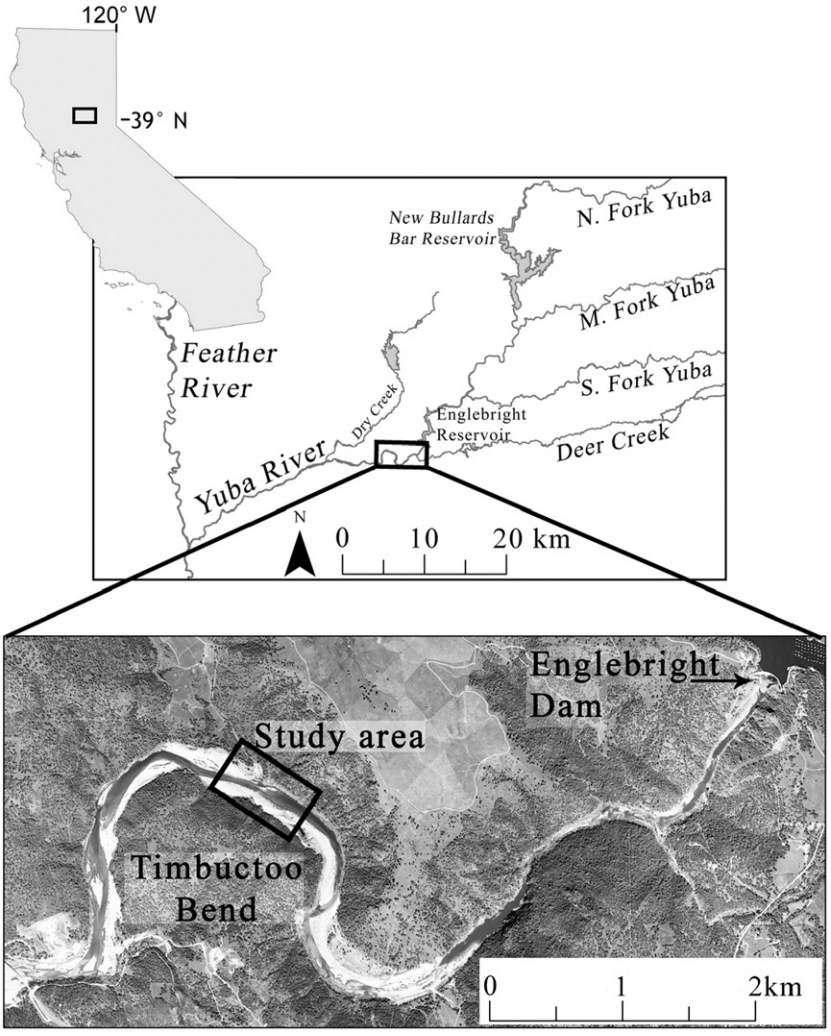

Fig. 1. Study area: Timbuctoo Bend on the Lower Yuba River, northern California, USA.

Middle Forks (Spaulding Dam and Jackson Meadows Reservoir), they are situated high enough in the watershed that their effects on flows (particularly during floods) in lower river locations are minimal. In contrast, New Bullards Bar Dam (operational in 1969) captures nearly the entire runoff of the North Fork Yuba and has a large reservoir capacity of 1.2 billion m^3 (6.7 times the combined total capacity of Spaulding and Jackson Meadows). Englebright Dam is an older concrete arch dam built in 1941 on the mainstem Yuba ~38 km upstream from the confluence with the Feather and ~16 km downstream from New Bullards Bar. It stands 85 m high in a narrow canyon, has a reservoir capacity of 86 million m^3, and primarily serves as a sediment barrier blocking export of hydraulically mined, gold-depleted sedimentary deposits. Although a smaller structure with limited impact to flood flows, it is very important to geomorphic and ecologic processes on the Yuba, being a complete barrier to the passage of sediment downstream and anadromous fish migration upstream. The section of the mainstem river from Englebright Dam downstream to the confluence with the Feather is defined as the Lower Yuba River (LYR). Although Englebright Dam was built with the purpose of trapping sediment liberated during hydraulic-mining operations, by the time it was built large volumes of material had already infilled the lower river valley to depths of up to 25 m. This large storage of sediment in the LYR is frequently reworked and provides a long-term template of channel incision.

The statistical "bankfull" discharges (~1.5-yr return interval of annual peak series) recorded at the U.S. Geological Survey (USGS) Smartville gauge (#11418000) located 0.5 km downstream of Englebright Dam for the periods 1942–2004 and for 1971–2004 are 330 and 160 $m^3\ s^{-1}$, respectively, illustrating the significant impact to hydrology of New Bullards Bar. Englebright Dam has a controlled flow release potential of 135 $m^3\ s^{-1}$, although uncontrolled flows over Englebright Dam occur frequently. One hundred flow events have exceeded bankfull discharge and overtopped Englebright Dam between the construction of New Bullards Bar Dam in 1970 and the beginning of October 2005. Over the 1971–2004 period, the median daily discharge at the Smartville gauge was 43.6 $m^3\ s^{-1}$. The 5-, 10-, and 50-yr return interval discharge for 1971–2004 are 1050, 1450, and 4025 $m^3\ s^{-1}$, respectively. Therefore, despite some flow regulation, the Yuba River below Englebright Dam experiences a dynamic flood regime. The combination of a near-natural flood hydrology and a plentiful supply of locally stored sediment in the LYR provides a

dynamic geomorphic environment that produces a sequence of active bar complexes and a heterogeneous channel and floodplain morphology normally associated with a wandering gravel-bed river.

2.1. Timbuctoo Bend study site

The specific site examined in the present study is located 6.3 km downstream from Englebright Dam within 'Timbuctoo Bend', a highly dynamic and active gravel/cobble zone of the river (Figs. 1 and 2). Timbuctoo Bend has a well-connected floodplain with large active gravel bars, secondary and tertiary flood channels, limited vegetation encroachment, and nonuniform channel geometry. Based on aerial photographs from 1937 to 2006, historical channel change has been dramatic, including emplacement of large dredger tailings on the floodplain, activation and abandonment of channels, and cycles of willow growth and natural levee stabilization. The study site is 460 m long and extends laterally ~300 m to include the entire valley floor up to the 50-yr return interval water surface elevation. In 2004 it was dominated by an island/bar complex that generally defined a pool-riffle-run sequence of morphological units in the downstream direction. Sediments are dominantly in the cobble (64–256 mm) and gravel (2–64 mm) size classes and exhibit spatial patterns that indicate hydraulic sorting during a period of few high flow events following a large flood in 1997 (~42-yr return interval). In recent years, this site is the most heavily utilized area of spawning habitat by Chinook salmon on the Yuba River.

Between the Smartville gage and the study site, a tributary (Deer Creek, USGS station #11418500) enters the river, contributing direct runoff during rain events and little otherwise. Deer Creek drains ~220 km^2 on the southeast margins of the Yuba Basin. Therefore, flood hydrographs at the study site during rainstorm events reflect the combined flow of the mainstem Yuba and Deer Creek.

3. Methods

3.1. Field methods

Field data were collected between April 2004 and April 2005, a period characterized by relatively stable flows (see Section 3.1.5). Conditions in the channel were documented using a combination of detailed topographic data, morphological classification, hydraulic measurements, sediment analysis (visual assessments and pebble counts), and spawning utilization surveys. Field data were used to develop and validate a two-dimensional hydrodynamic model, and then model results were used to characterize high-resolution hydraulic patterns at the mesoscale and how this relates to spawning activity.

3.1.1. Topography

A detailed map of channel topography was used to aid geomorphic interpretation and to describe the bottom boundary for the two-dimensional hydrodynamic model. The map was obtained using a similar method to Brasington et al. (2000), Pasternack et al. (2004) and Elkins et al. (2007); a Topcon GTS-802A robotic total station measured bed positions on a staggered grid with supplemental points as needed to resolve bed features (e.g., boulders, slope breaks, etc.). The mean sampling density in the channel was 0.61 points m^{-2}, with a lower density on the

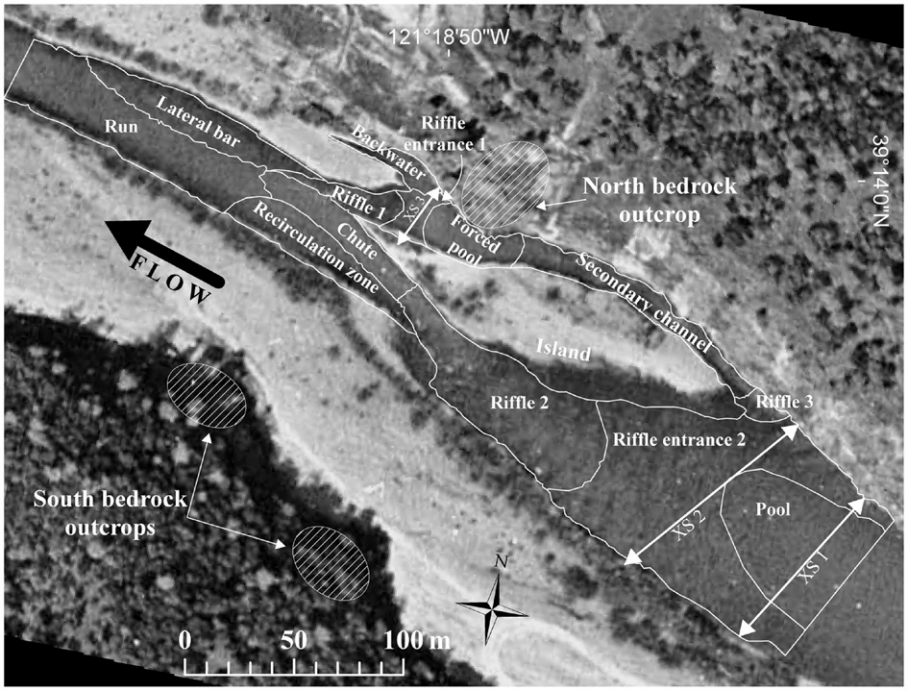

Fig. 2. Aerial photograph of the study site showing the extent of the modelled reach, the identified morphological units and the location of the hydraulic validation cross-sections. The mismatch between the modelled and photograph water edge reflects different discharges (23.4 m^3 s^{-1} modelled, ~30 m^3 s^{-1} photo).

relatively flat floodplain. Surveying accuracy was assessed using 98 control network checks and was found to average 0.013 m in the horizontal and 0.011 m in the vertical, which is significantly smaller than the natural error induced by the bed material, typically ranging in size between 0.05 and 0.2 m.

3.1.2. Morphological units

Morphological units were identified by expert-based reconnaissance of the site during detailed topographic surveying and through interpretation of features evident in the Digital Elevation Model (DEM, discussed in Section 3.2). No definitive morphological unit classification scheme was identified in the literature. Therefore, the scheme adopted represented a combination of morphological definitions (e.g., Montgomery and Buffington, 1997; Padmore et al., 1998; Thompson et al., 2001) specifically adapted for the characteristics of the study site. The geomorphic unit classifications used at the site were pool, riffle, run, riffle entrance, forced pool, chute, lateral bar, recirculation zone, backwater, and secondary channel, each of which are described in Table 1. Only two unit types were replicated at the study site; there were three riffles and two riffle entrances. For statistical purposes it would have been preferable to have had a number of replicates of each unit type. However, this would have meant modeling a much larger section of the river to obtain even one replicate of every unit type, especially since the study site had a highly diverse morphology within the context of the LYR. This would not have been practical given the resolution of data required for the objectives of the study.

Clearly, classification procedures that integrate underlying topography with surface flow are intrinsically linked to hydrological regime. As discharge increases, the spatial distribution of relative hydraulic conditions will vary. Hydraulic heterogeneity also tends to decrease with increasing discharge (Stewardson and McMahon, 2002; Moir et al., 2006; Brown and Pasternack, in press) with the associated merging and simplification of morphological/habitat units. However, the classification of morphological units in this study was carried out during the spawning season and therefore represents a relatively narrow discharge range (see Section 3.1.5) with little potential for variation in the spatial distribution and classification of morphological units.

3.1.3. Hydraulics

Cross-sectional depth and velocity data were collected along three transects (Fig. 2) on February 13, 2005 using standard methods appropriate for validating a two-dimensional hydrodynamic model (Wheaton et al., 2004a; Pasternack et al., 2004, 2006; Brown and Pasternack, in press). The only modification of the method for this study (on a much wider river) was to use the Topcon GTS-802A to survey the exact position of each paired measurement of depth and velocity, which were collected an average spacing of 2.87-m along a transect. This allowed field data to be precisely compared to model predictions for the same location. Transects 1 and 2 span the mainstem channel and were also used to estimate total discharge, whereas transect 3 spanned only the side channel. Measurement errors were ±1 cm for depth using a stadia rod and ±33 mm s^{-1} root mean square for velocity using a Marsh-McBirney Flo-Mate 2000. Velocity was sampled at 30 Hz and averaged over 30 s at 0.6 × depth from the water surface to obtain a measure of the depth-averaged velocity. Measuring velocity at one position within the water column was appropriate given the uniform flow conditions and low relative bed roughness (water depth was 10–20 × local median substrate size, d_{50}) in the location of the three transects. Studies of flow around individual large grains and pebble clusters demonstrate that point measurements of velocity at arbitrary locations on a gravel bed will be strongly influenced

Table 1
Description of morphological unit types identified at the study site

Morphological unit	Description
Pool	A region of relatively deep and slow flow with low water surface slope.
Riffle	Relatively fast and shallow flow with high water surface slope and rough water surface texture. Such units may be associated with the downstream face of a transverse (alternate) bar feature.
Riffle entrance	A transitional zone between an upstream pool and downstream riffle. Water depth is relatively low and velocity characterized by a downstream convective acceleration toward the riffle crest that is often associated with lateral and vertical flow convergence. The upstream limit is at the approximate location where there is a transition from a divergent to convergent flow pattern. The downstream limit is at the slope break of the channel bed termed the riffle crest.
Run	Exhibits a moderate flow velocity, low to moderate depth, and moderate water surface slope. Such units typically exhibit a moderate to high roughness of water surface texture and tend not to be associated with transverse bar features that riffles may be.
Forced pool	A subclass of pool in which a localized area of the bed is "over-deepened" from local convective acceleration and scour associated with static structures such as woody debris, large boulders, or bedrock outcrops (Montgomery and Buffington, 1997; Thompson et al., 2001).
Chute	Characterized by the moderate flow velocity and relatively high depth of the channel thalweg. Chutes are often located in a constriction downstream of a riffle as it transitions into a run. Chutes typically have relatively coarse sediment.
Lateral bar	A depositional unit that is located at the channel margins and orientated longitudinally to the direction of flow. The feature slopes toward the channel thalweg with an associated increase in both flow depth and velocity. Sediment size tends to be lower than in adjacent sections of the channel.
Recirculation zone	Characterized by low-velocity or recirculating flow, often bound by a hydraulic shear zone toward the channel thalweg that controls flow separation and the shedding of turbulent eddy structures. These units are usually the associated with an abrupt transition in the topography of the channel (e.g., the downstream extent of a bar feature or bedrock outcrop) that results in lateral flow separation.
Backwater	An area of low-velocity flow adjacent to the main channel but connected at the downstream or upstream end of the unit.
Secondary channel	A smaller channel active under normal flow conditions that is connected at both upstream and downstream ends to the mainstem channel. In reality such features may incorporate a range of morphological characteristics, but in order to be classified at the same absolute resolution as is necessary for mainstem units, a single unit is defined. These units therefore tend to extend over a greater dimensionless length (i.e., number of channel widths) than others.

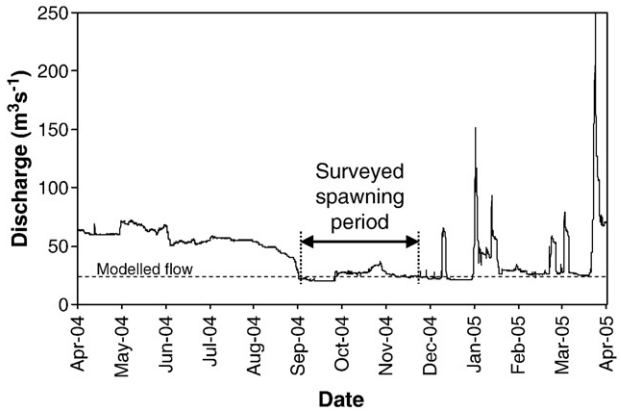

Fig. 3. Hydrograph for the study period (i.e., April 2004 to April 2005). The period over which spawning analyses were carried out is highlighted. The horizontal dashed line represents the modeled discharge (25.7 $m^3 s^{-1}$ as indexed to combined USGS flow data from the Yuba River and Deer Creek).

by these features at the 0.1–0.5 m scale (Acarlar and Smith, 1987; Paola et al., 1986; Kirkbride and Ferguson, 1995; Buffin-Belanger and Roy, 1998; Lawless and Robert, 2001a,b).

3.1.4. Sedimentary analysis

The general sedimentary characteristics across the entire site were visually assessed and mapped. This data was subsequently linked to the individual morphological units identified at the site (Section 3.3.1). In this procedure, sediment character was defined in terms of the dominant and subdominant size classes (i.e., boulder > 256 mm, cobble 64–256 mm, gravel 2–64 mm, sand and finer < 2 mm, all sizes being intermediate axis diameter).

Using the "Wolman-walk" procedure (Wolman, 1954), 32 pebble counts were also conducted at the study site. Although they were all carried out under low discharge conditions, flows at certain regions of the site were too deep and/or fast to permit sampling using this technique. Thus, samples were not evenly distributed throughout the site or across all morphological units; they tended to be biased toward accessible channel margin locations. Therefore, only backwater, recirculation zone, riffle entrance and run units were sampled. At each location, a minimum of 100 particles (mean = 120, range = 100–219) were sampled across a ~3 × 3 m section of the bed. The position of the center point of each sampling location was surveyed using a Topcon GTS-802A robotic total station.

3.1.5. Redd mapping

The location of individual redds (cumulative total = 451) were surveyed on 52 days between September 17 and November 16 inclusive during the 2004 spawning season by experienced observers. The location of the deepest part of the redd "pit" was surveyed in each case using a Topcon GTS-802A robotic total station. Redds that had been previously surveyed were identified by a painted marker stone that was placed in the pit. If the marker stone was buried by subsequent redd excavation, the position of the modified pit was re-surveyed. There are 'spring' and 'fall' runs of Chinook spawn in the LYR, with both spawning in the fall. Some local experts identify spring run fish as those that spawn September 1–30 and fall run from October 1 to December 31 in the Yuba, while others disagree with this delineation and report overlap in timing so that it is difficult to tell with certainty that a given redd was constructed by spring or fall fish. In relation to the period of spawning surveying undertaken in this study, the nominal "spring run" could be considered to have been sampled September 17 to 30 and the "fall run" from October 1st to November 16. However, the first survey carried out on September 17 mapped all the redds that had been constructed prior to that date. During this initial survey there were still relatively few redds at the site and it was apparent that each was a discrete feature (i.e., there was no evidence that superimposition had occurred by that point). It was therefore unlikely that many redds constructed prior to September 17 were not identified. Thus, redds were effectively mapped between the onset of the 2004 spawning season and November 16. Although fall spawning is regarded to continue until December 31, the cumulative number of redds was so high in the 2004 spawning season that by mid-November it was very difficult to distinguish between new and previously constructed redds, despite the use of markers to identify previously mapped features. Therefore, to avoid bias through re-sampling, the final redd survey was conducted on November 16. The number of redds surveyed by that date (i.e., 451) was sufficient to conduct subsequent statistical analyses. Subsequent visits to the study site after November 16 revealed that no new locations had been utilized so that the spatial cover of the surveys conducted was representative. Over the period September 1 to November 16, discharge was well below bankfull (160 $m^3 s^{-1}$) and relatively stable compared to the variation over the period April 2004 to April 2005 (Figs. 3 and 4). Spawning period non-exceedence probability values for daily discharge, Q_{10}, Q_{50}, and Q_{90}, were 30.2, 25.4, and 20.0 $m^3 s^{-1}$, respectively (Fig. 4). Flow variations were due to dam releases that delivered water to downstream users. There was some variation in flows between the periods September 1 to 30 and October 1 to November 16, with median and mean discharge values of 20.6 and 21.7; and 26.8 and 27.3 $m^3 s^{-1}$, respectively.

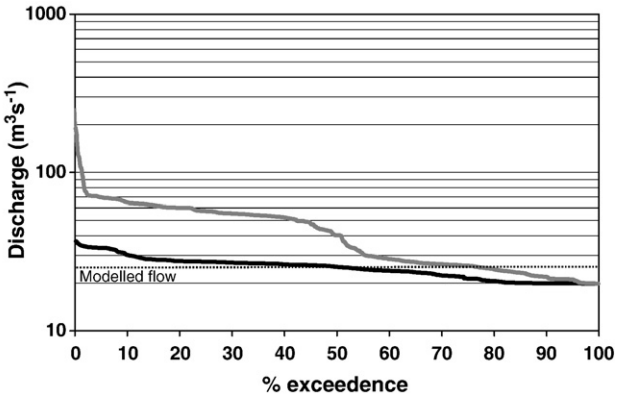

Fig. 4. Flow duration curves for the study period (i.e., April 2004 to April 2005; solid grey line) and spawning analysis period (solid black line). The horizontal dashed line represents the modeled discharge (25.7 $m^3 s^{-1}$ as indexed to combined USGS flow data from the Yuba River and Deer Creek).

3.2. Two-dimensional Yuba model

Two-dimensional (depth-averaged) hydrodynamic models have existed for decades and have been used to study a variety of hydrogeomorphic processes (Bates et al., 1992; Leclerc et al., 1995; Miller and Cluer, 1998; Cao et al., 2003). Recently, they have been evaluated for use in regulated river rehabilitation emphasizing spawning habitat restoration by gravel placement (Pasternack et al., 2004, 2006; Wheaton et al., 2004b; Elkins et al., 2007) and to better understand the relative benefits of active river rehabilitation versus flow regime modification (Jacobson and Galat, 2006; Brown and Pasternack, in press) on regulated rivers. In this study, the long-established two-dimensional model known as Finite Element Surface Water Modeling System 3.1.5 (FESWMS), implemented within the Surface-water Modelling System (SMS) graphical interface (Environmental Modeling Systems, Incorporated), was used to simulate site hydrodynamics at the 1-m scale relevant to microhabitat utilization by fish that are ~1 m long. FESWMS solves the vertically integrated conservation of mass and momentum equations using a finite element method to acquire depth-averaged two-dimensional velocity vectors and water depths at each node in a finite element mesh (Froehlich, 1989). A mesh element is "dry" when depth is below a user-defined threshold (set at $1 \times d_{90} \sim 0.12$ m here), but to the extent possible, the mesh area was trimmed to closely match the observed wetted area.

FESWMS is a long-established model best viewed as a conceptual guide of likely outcomes, rather than literal truth. Application of FESWMS to gravel-bed rivers has been extensively validated on the Lower Mokelumne River (four basins south of the Yuba and having similar spawning period discharge and bed material conditions) using observed velocity and depth at 35 cross-sections. This indicated good predictions for the gravel bed and poor predictions around large woody debris or complex banks (Pasternack et al., 2004, 2006; Wheaton et al., 2004a; Elkins et al., 2007). Pasternack et al. (2006) reported details regarding FESWMS model uncertainty when used for gravel-bed rivers. They found that FESWMS could predict local shear stress over gravel-bed riffles as accurately as five common field estimation methods. MacWilliams et al. (2006) compared FESWMS with one-dimensional and three-dimensional models of gravel-bed river hydrodynamic and found that the two-dimensional model was capable of simulating key stage-dependent processes responsible for riffle-pool maintenance. Details on the validation procedure used in this study follow the explanation of model development.

3.2.1. Model development

Topographic data were imported into Autodesk Land Desktop 3 to create a digital elevation model (DEM) of the study site using a standard approach (Wheaton et al., 2004a; Pasternack et al., 2004, 2006; Elkins et al., 2007). Refined topographic point and break-line data used to produce the DEM were exported to SMS for use in the two-dimensional model. The two-dimensional mesh was generated using a built-in paving algorithm without reference to the independently located depth and velocity measurement points. This independence provided a fair test of the accuracy of a two-dimensional model without special attention to the mesh in the vicinity of validation locations. Node elevations were interpolated from imported DEM data using a Triangulated Irregular Network (TIN)-based scheme. The wetted mesh covered 24,483 m^2 of channel with 51,000 computational nodes comprising 24,847 elements, with the highest density near boulder clusters. The node density of the mesh varied but averaged 2.1 points m^{-2}, which was higher than that for the DEM.

To run FESWMS, discharge and downstream boundary water surface elevation were obtained from velocity–area flow gauging and by surveying the water surface edge, respectively. Based on an analysis of combined USGS gage data from the Yuba at Smarville and Deer Creek, simulations were made for the minimum, median, and maximum discharges during the spawning period. For sake of brevity and recognizing from preliminary comparisons of model output that the median flow was representative of the discharge range over the spawning season, only results associated with the median flow simulation are presented and analyzed. For that median flow, the field-measured discharge was 23.4 $m^3\ s^{-1}$, which is the mean of discharges calculated at the two channel-wide cross-sections measured in this study. This corresponded to a combined flow of 25.7 $m^3\ s^{-1}$ from the upstream USGS gages (Smartville and Deer Creek). The 9% difference is thought to be due to transmission losses between the USGS gages located in bedrock reaches and the study site located on thick hydraulic-mining deposits of permeable gravel. The water surface elevation corresponding to the modeled discharge at the downstream end of the site was surveyed by total station with a vertical accuracy of ±2 cm and found to be 66.25 m relative to the NAVD88 vertical datum.

Rather than calibrating the model to obtain optimal parameters that might be physically unrealistic, the approach taken was to estimate parameters using field data and then validate the resulting model predictions to assess the resulting accuracy. The two primary model parameters in FESWMS are bed roughness (as approximated using Manning's n for a gravel/cobble bed) and isotropic kinematic eddy viscosity (E). The effect of channel roughness on flow was addressed two ways in the model. Roughness associated with resolved bedform topography (e.g., rock riffles, boulders, gravel bars, etc.) was explicitly represented in the detailed channel DEM. Two-dimensional model predictions are highly sensitive to DEM inaccuracies (Bates et al., 1997; Hardy et al., 1999; Lane et al., 1999; Horritt et al., 2006), which is why detailed topographic mapping was done in this study. For unresolved roughness, Manning's coefficient (n) was estimated as 0.043 for the gravel-bed area with $d_{50} \sim 50$ mm and 0.06 for the coarse cobble/boulder bed over the highest velocity section of the riffle using a standard linear summation method (McCuen, 1989). Although it is possible to vary the bed-roughness parameter spatially in a two-dimensional model to try to account for variable bed sediment facies, it is difficult to justify small (<0.005) local deviations relative to two-dimensional model and measurement accuracy in gravel-bed rivers. Two-dimensional models have

been reported to be sensitive to large (>0.01) variations in n values (Bates et al., 1998; Lane and Richards, 1998; Nicholas and Mitchell, 2003), and the validation approach used here would reveal that scale of deficiency.

Miller and Cluer (1998) showed that two-dimensional models could be particularly sensitive to the eddy viscosity parameterization used to cope with turbulence. In the model used in this study, eddy viscosity (E) was a variable in the system of model equations, and it was computed using the following standard additional equations developed based on many studies of turbulence in rivers (Fischer et al., 1979; Froehlich, 1989):

$$E = 0.6H \cdot u_* + E_0 \tag{1}$$

$$u_* = U\sqrt{C_\mathrm{d}} \tag{2}$$

$$C_\mathrm{d} = 9.81\frac{n^2}{H^{1/3}} \tag{3}$$

where H is water depth, u_* is shear velocity, U is depth-averaged water velocity, C_d is a drag coefficient, n is Manning's n, and E_0 is a minimized constant (0.033 $m^2\ s^{-1}$) necessary for model stability These equations allow E to vary throughout the channel, which yields more accurate transverse velocity gradients. However, a comparison of two and three-dimensional models for a shallow gravel-bed river demonstrated that even with this spatial variation, it is not enough to yield as rapid lateral variations in velocity as occurs in natural channels, presenting a fundamental limitation of two-dimensional models like FESWMS (MacWilliams et al., 2006).

3.2.2. Model validation

Recognizing that two-dimensional models, like all models, have inherent strengths and weaknesses, some amount of uncertainty in model results must be understood and accepted (Van Asselt and Rotmans, 2002). Since model parameters were set to physically realistic values and not numerically calibrated to match observations, comparisons of predicted and observed conditions provide a meaningful assessment of model parameter uncertainty. Three different types of validation testing were done to evaluate model performance at 23.4 $m^3\ s^{-1}$, making use of the depth and velocity data collected at three cross-sections as well as water edge elevations collected around the perimeter of the site.

First, to test the suitability of the selected Manning's n values of 0.043 and 0.06, the Topcon total station was used to measure the longitudinal profile of water surface elevation along the reach at 23.4 $m^3\ s^{-1}$. Over the 460 m length of channel, 113 measurements were made at a ~4-m interval. The deviations between the observed and model-predicted values were calculated and statistically described.

Second, to validate model performance with regard to the key model parameter of eddy viscosity, the range of E values in model output was checked against field-based estimates. Field estimates of E were calculated using Eqs. (1)–(3) with observed depth and velocity measurements at the study's cross-sections, except that no E_0 value was needed. The mean and range of E values were compared between model predictions and field-based estimates. Also, a qualitative evaluation was made to determine if the model correctly predicted flow recirculations behind boulders and bedrock outcrops where they were visually evident during field observations, which is controlled by the model's E values.

Third, to quantify the accuracy of depth and velocity predictions at points and across the three cross-sections, total station surveyed coordinates of each field measurement of depth and velocity were imported into SMS, and then model depths and velocities at those exact locations were obtained using TIN-based interpolation of model result at computational nodes. For a simple point-scale comparison, matching data and predictions were statistically evaluated without any spatial context. To better comprehend the spatial pattern of observed versus model-predicted velocities across a channel, it is helpful to discern sub-grid scale spatial fluctuations from grid-resolvable trends. This was achieved by fitting a cross-sectional smoothing curve to the data using the locally weighted Least Squared error method and then comparing the two-dimensional model predictions to the smoothed curve. The fraction of the data considered during each smoothing step was set to 20%, thus for cross-section 3 where there were fewer measurement points, smoothing was minimal.

3.3. Data analysis

3.3.1. Morphological unit hydraulics

After characterizing model accuracy, depth and velocity were extracted from the two-dimensional model output and used to characterize morphological units. Depth and velocity data were not non-dimensionalized (e.g., by grain size) since this would likely have obscured important relationships linked to the absolute sedimentary and hydraulic habitat requirements of spawning salmonids that are linked to their body size (Crisp and Carling, 1989). Rather, the Froude number was adopted as a non-dimensional parameter to test for differences in the hydraulic characteristics between morphological units. It was calculated from the basic model output data at each node from the relationship:

$$\mathrm{Fr} = \frac{U}{(H \cdot g)^{0.5}} \tag{4}$$

where g is gravitational acceleration (9.81 $m\ s^{-2}$). Since it is dimensionless, the Froude number provided a scale-independent means to discriminate between morphological unit classes in terms of their hydraulic character. Hydraulic data were returned to the spatial resolution of the surveyed data (i.e., 0.61 points m^{-2}) from that of the higher point density of the model grid (i.e., 2.1 points m^{-2}). This was done by employing a random filter of the data that reflected the proportional difference in the spatial point densities. The predicted depth, velocity, and Froude number values for all model nodes were distributed into subsets corresponding to the classified morphological units (Fig. 2).

Between-subset differences in the overall distribution of the Froude number (i.e., the shape of cumulative frequency

distributions rather than just comparing the variance or mean) were carried out using the Kolmogorov–Smirnov (K–S) test. The values of the K–S statistic were used to provide an indication of the relative similarity/difference in hydraulic (Froude number) characteristics between morphological unit pairings at the study site. The 10th and 90th percentiles of the K–S values were arbitrarily used to define hydraulically similar and different morphological unit pairings, respectively. In this way it could be examined whether morphological units with the same classification exhibited more similar Froude number distributions than differently classified units and if differently classified unit types had similar Froude number characteristics.

To summarize the joint depth–velocity distribution of the identified morphological units, a statistical classification procedure (Kernel Discriminant Analysis, KDA) was used. Since the hydraulic data for each unit tended not to be normally distributed, a confidence limit based contouring approach could not be adopted. KDA objectively assessed the hydraulic character of the identified morphological units by comparing each data point to every other data point (i.e., using a cross-validation method) and determining which morphological unit it was most likely to be associated with, via a probabilistic measure. The data are summarized by actual unit class (i.e., the morphological unit that model output data was assigned to based on their spatial distribution, Fig. 2) in terms of the proportion of points within each morphological unit class as predicted by KDA. In effect the procedure calculates the morphological unit classes that are most probable to occur across the entire depth–velocity hydraulic space.

3.3.2. Abiotic–biotic integration

Individual surveyed redds were assigned to subsets corresponding to the classified morphological units. The depth, velocity, and Froude number values at the location of each redd were obtained from two-dimensional model output using ArcGIS 9.0. Utilization frequency was standardized by the area of respective morphological units to produce mean redd density within a unit (redds·m^{-2}). A morphological unit suitability index (MUSI) was calculated by employing the relativized electivity index (Vanderploeg and Scavia 1979; Lechowicz, 1982). This index discriminates equally between selection and avoidance (in this case of morphological unit types) and is calculated with the equation:

$$E^* = \frac{\left(\frac{R}{\sum R}\right) - \frac{1}{n}}{\left(\frac{R}{\sum R}\right) + \frac{1}{n}} \quad (5)$$

where R is the ratio of the proportions of utilization to availability for each unit type and n is the number of unit types. E^* varies between −1 (avoidance) and +1 (selection) with 0 representing indifference. A value of MUSI > 0 indicates a greater proportional utilization than availability of a particular unit and therefore "selected" or "preferred" by spawning fish. A MUSI value of 0 indicates utilization proportional to availability, between −1 and 0 indicate "tolerated" conditions (i.e., fish utilize the unit but at a proportion lower than that unit's availability) and values of −1 (i.e., no utilization), "avoided". MUSI values of all the morphological units were regressed against each of the median hydraulic descriptors (i.e., H_{50}, U_{50}, and Fr_{50}).

4. Results

4.1. DEM and morphological units

Within the general pool-riffle-run pattern of the study site, transitional units (riffle entrances and a chute) and laterally discrete units (lateral bar, recirculation zone, secondary channel and backwater) were identified that added heterogeneity (Fig. 2). Only the center section of the secondary channel was provided with that specific classification (i.e., secondary channel) because more discretely defined units were identified at the upstream (riffle) and downstream (forced pool, riffle entrance, and riffle) margins. At this resolution it is apparent that the large bedrock outcrop at the north channel margin near the centre of the modeled reach (Fig. 2) is likely responsible for the development of the adjacent forced pool

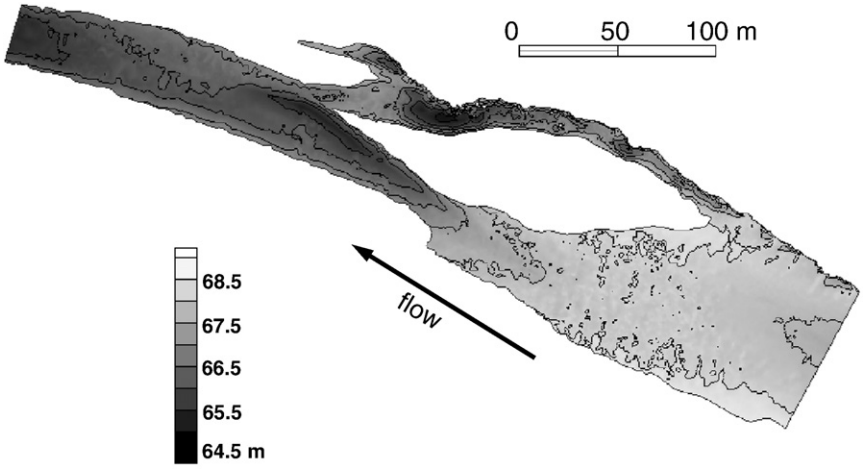

Fig. 5. DEM of the Timbuctoo Bend study site, Lower Yuba River.

unit (Fig. 5). The DEM highlights the variation in channel geometry through the study site. The channel initially widened from 80 m at the pool at the upstream limit of the site to 100 m at the head of the island feature where the mainstem and secondary channels diverge. The mainstem channel then narrowed sharply (85 m wide at the channel split to 15 m at the narrowest point of the riffle) before widening again towards the tail of the island (30 m at the island terminus). Once the secondary channel rejoined the mainstem downstream of the island, width increase to a maximum of 40 m before reducing to 30 m at the downstream limit of the study site.

4.2. Model validation

Three types of validation were carried out to understand the uncertainty in the two-dimensional model. The first validation test was a comparison of observed and predicted longitudinal water surface profiles to assess the validity of the Manning's n values used. The modeled water surface elevation was slightly lower than observed for 76% of the test points. Of these, the median deviation was 0.046 m. For those 24% of points whose predicted water surface elevation was higher than the observed value, the median deviation was only 0.023 m. Among all points, half were within 0.04 m and 90% within 0.11 m. Given water depths ranged from 0–2.6 m and an observational measurement error at control point checks of 0.011 m, the deviation between model predictions and observations was considered acceptable.

The second validation test was an assessment of E values between model predictions and field-based estimates. The resulting mean (0.057 $m^2\ s^{-1}$) and range (0.034–0.075 $m^2\ s^{-1}$) of model E values were higher than the field-based estimates (0.023 and 0.001–0.043 $m^2\ s^{-1}$), but proved low enough to yield recirculating eddies in the model behind boulders and bedrock outcrops. The difference in modeled and measured values of E introduces extra momentum transfer and decreases velocity gradients in model results, as reported in a comparison of two and three-dimensional models by MacWilliams et al. (2006).

The third validation test was an assessment of the accuracy of depth and velocity predictions at points and across the three cross-sections. Hydraulic conditions at all of the points ($n=83$) along three cross-sections showed reasonable matching of predicted versus observed depths and velocities, typical of two-dimensional models (Fig. 6). First, consider only the raw observations and model predictions. An overall comparison of raw observed versus predicted values among all 83 points found a coefficient of determination of 0.929 for depth and 0.768 for velocity ($P<0.001$ for both tests). The average absolute deviation between raw observed and predicted depth was 10%, which is consistent with the deviations in water surface elevations reported above. Excluding one anomalously low measured value at the 80 m mark of cross-section 1 (Fig. 6), the average absolute deviation between raw observed and predicted velocity was 22%, which is typical given the variability inherent in stream measurements. The maximum error observed between an individual raw observation and corresponding model-predicted value was 66% for depth and 213% for velocity, highlighting the importance of sub-grid scale spatial fluctuations to field measurements.

Since the scale of an adult spawner and a redd is at the grid-scale or larger, it is valuable to filter out spatial measurement "noise" (i.e., sub-grid scale fluctuations) and see how the model performed in matching grid-resolvable cross-channel trends in depth and velocity compared to the smoothed observational trends. For cross-section 1, both depth and velocity predictions closely match the smoothed best-fit curve of the observed data. Depth and velocity values at cross-section 2 show more lateral variation than at cross-section 1, with the predicted pattern following the observed pattern, but not matching it as tightly (e.g., deviation of 0–40% for velocity). At cross-section 3, the model under-predicted depth in the north half of the channel and over-predicted it in the south while generally over-predicting velocity, but the spatial patterns matched closely. No statistically significant correlation existed between the magnitudes of depth and velocity errors across all data, indicating that the high-resolution DEM was very high quality and not responsible for the resulting errors, as previously reported for such models (Pasternack et al., 2004, 2006). Similarly, since depth is not consistently over or under-predicted across the section, uncertainty in Manning's n cannot be responsible. Based on a comparison study of one, two, and three-dimensional models of a different gravel-bed river (MacWilliams et al., 2006), the most likely explanation is that eddy viscosity is not varying enough spatially, causing too much momentum transfer across the channel and thus smoothing the velocity field. Further decreasing E_0 to enhance spatial variability in eddy viscosity causes model instability, so this ultimately is the limiting factor in the accuracy of two-dimensional models. Overall, the two-dimensional Yuba model using realistic parameters provided good depth and velocity prediction and performance comparable to or better than the accuracies reported for other two-dimensional modeling studies (e.g., Lane et al., 1999; Rathburn and Wohl, 2003; Gard, 2006; Pasternack et al., 2006; Elkins et al., 2007; Brown and Pasternack, in press).

4.3. Model output and hydraulics of morphological units

Model predictions of the spatial distribution and magnitude of depth, mean column velocity, and Froude number are provided in Fig. 7A–C, respectively; summaries of hydraulic output by morphological unit type are given in Table 2. Although hydraulic conditions were highly variable across the entire site, broad flow patterns reflected underlying channel topography. A general sequence of flow divergence–convergence–divergence–convergence is observed in a downstream direction through the site, the pattern reflecting variations in channel cross-sectional area described in Section 4.1. Flow accelerated and shallowed between the upstream limit of the site and the topographic high of the riffle crest. Further convective acceleration occurred through the relatively steep riffle 1 unit, accentuated by the lateral constriction of the channel in this region and resulting in the highest velocities throughout the site for the modelled flow (mean column velocity = 3.1 $m\ s^{-1}$).

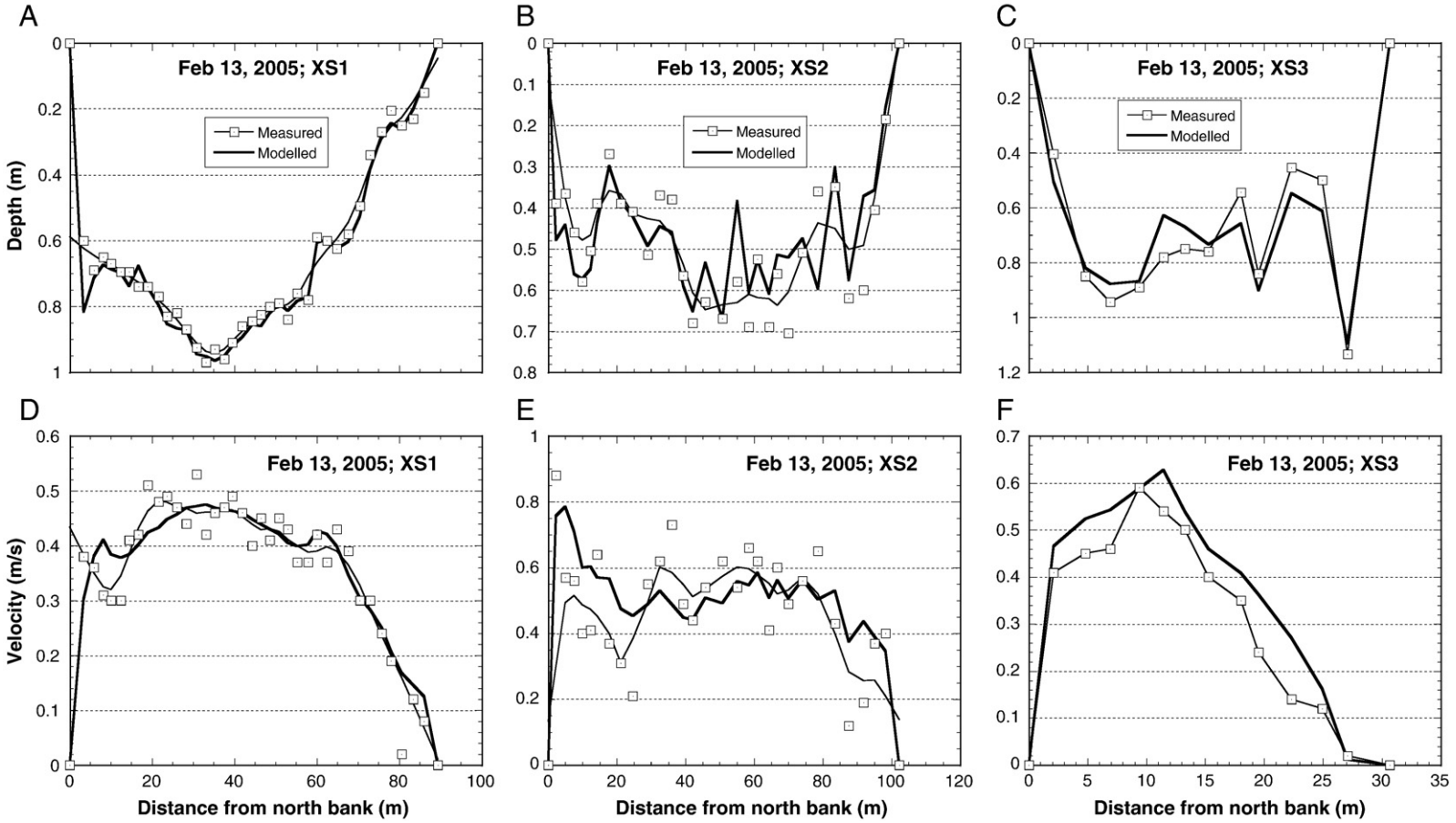

Fig. 6. Comparisons of observed versus predicted (A) depths and (B) velocities at three representative cross-sections. Field observations were fit with a curve using the locally weighted least squared error method to reduce measurement noise.

Downstream of the location where the mainstem and secondary channels rejoin the flow again shallowed and subsequently deepened (with mutual increases and decreases in velocity) as it passed the topographic high associated with the lateral bar unit, the feature also forcing the thalweg towards the south bank.

4.3.1. Froude number characteristics of morphological units

The Froude number distributions of the morphological units show a wide range, with median values varying from 0.001 in the backwater to 0.63 in riffle 1 (Fig. 8; Table 2). Table 2 also shows that specific units exhibited a wide range in Froude number (e.g., riffles 1,2 and 3 had a 5th to 95th percentile *Fr* range, Fr_{5-95}, of 0.73, 0.82 and 1.08, respectively, with a mean of 0.88) while others of a similar geographical area had small ranges (e.g., the pool unit had $Fr_{5-95}=0.06$). Similar morphological units had similar *Fr* characteristics. The three riffle and two riffle entrance units had similar within-type Fr_{50} values and 25th to 75th percentile ranges (Fig. 8, Table 2).

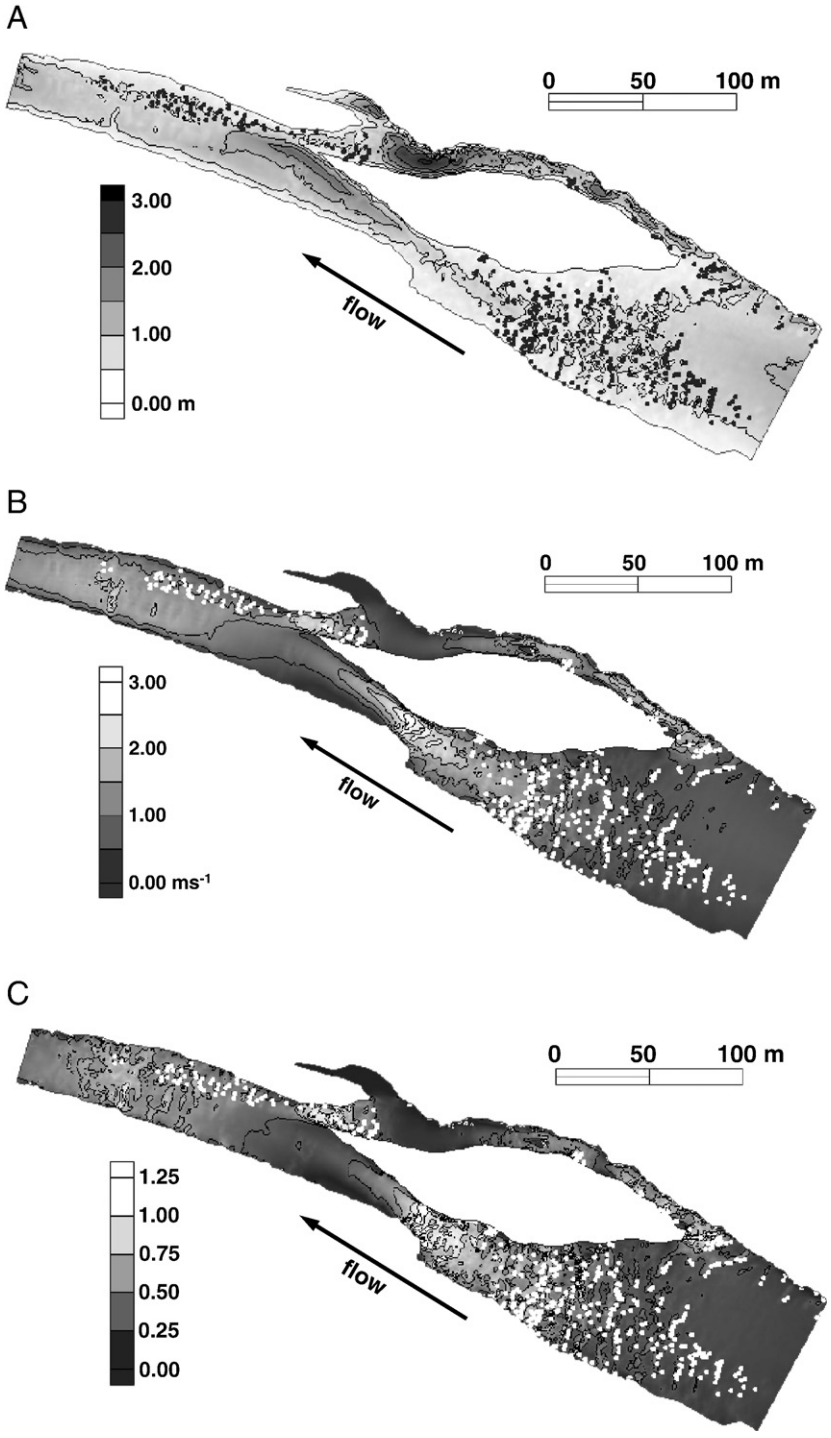

Fig. 7. Model output at the representative spawning period flow (23.4 $m^3\ s^{-1}$): (A) depth, (B) mean column velocity, (C) Froude number. Solid circles indicate the location of surveyed redds.

However, riffle entrances 1 and 2 versus chute and lateral bar versus run units display little difference in Fr_{50} and 25th to 75th percentile ranges despite having contrasting morphological classifications.

The results of the K–S test comparing the Froude number distributions of all the pairing combinations of morphological units are given in Table 3. The unit pairs that were most hydraulically similar and different to one another (defined by the 10th and 90th percentiles of the distribution of the K–S statistic values, respectively), are highlighted in Table 3 by bold and italic text, respectively. These data correspond with that presented graphically in Fig. 8; (i) units with the same morphological classification (i.e., the three riffle units and the two riffle head units) had similar Froude number characteristics, (ii) certain differently classified units (e.g., riffle entrance 1 and chute, run and lateral bar) appear hydraulically similar in terms of Froude number, and (iii) pool and forced pool units are consistently the most hydraulically different to other morphologies (including each other).

4.3.2. Depth–velocity hydraulic domain characteristics of morphological units

Fig. 9A–C summarizes the hydraulic domain of the morphological units, plotting the results of the KDA. The plots represent the regions of the hydraulic domain that can be probabilistically assigned to a specific morphological unit class. To aid visualization, the plots are divided into: a) averaged "preferred" versus "avoided" hydraulic domains (as defined by the MUSI statistic, Table 2), b) individual "preferred" morphological units, and c) individual "avoided" morphological units. In order to highlight the contrasting hydraulics between units exhibiting different utilization regimes by spawning salmon, the plots do not incorporate "tolerated" morphological units (i.e., pool and secondary channel units, Section 4.5). There is a very clear delineation between "preferred" and "avoided" morphological units; "preferred" units occupy a wide velocity range but relatively low depths while the opposite is the case for "avoided" units. In terms of the within-unit spread, riffles (collectively) and forced pool units are most heterogeneous (i.e., they cover a larger area of the depth–velocity space). In contrast, riffle entrance units (which combined accounted for the largest geographical area at the site, Table 2) extended over a relatively limited depth–velocity space; i.e., they exhibited relatively homogeneous hydraulic characteristics. It is also apparent that certain units exhibited discontinuous distributions across the depth–velocity space (e.g., lateral bar, Fig. 9B; run, Fig. 9C). The relative proximity of the hydraulic domains of different units generally agrees well with the K–S statistic used to indicate similarity in Froude number characteristics (Table 3). However, the two-dimensional nature of the plot allows the units that appear hydraulically similar in terms of Froude number characteristics (e.g., lateral bar and run, chute and riffle entrances, Fig. 8) to plot in discrete locations. Moreover, units that have the same morphological classification (i.e., riffles 1–3 and riffle entrances 1 and 2) remain within similar locations of the hydraulic domain.

The results of the KDA are also summarized in Table 4. In each case, the unit with the highest proportion of predicted points corresponds to the actual unit those points occur within (i.e., the morphological unit they were assigned to from the spatial unit classification, Fig. 2). Also, in five out of the ten types, the unit

Table 2
Summary of hydraulic, sedimentary and spawning data by morphological unit type

Descriptor	Backwater	Recirculation zone	Chute	Lateral bar	Pool	Riffle 1	Riffle 2	Riffle 3	Riffle entrance 1	Riffle entrance 2	Run	Forced pool	Secondary channel
H_{50} (m)	0.48	0.73	1.18	0.39	0.75	0.42	0.42	0.41	0.57	0.44	0.69	1.46	0.79
H_{5-95} (m)	1.40	1.04	1.42	0.55	0.40	0.58	0.77	0.95	0.69	0.56	0.87	2.10	1.36
U_{50} (m s^{-1})	0.002	0.44	0.73	0.85	0.45	1.19	1.06	1.32	0.53	0.46	1.13	0.29	0.86
U_{5-95} (m s^{-1})	0.10	0.81	1.14	1.02	0.12	1.35	1.67	1.58	0.81	0.85	1.15	0.50	1.54
Fr_{50}	0.001	0.17	0.21	0.43	0.16	0.63	0.53	0.56	0.22	0.22	0.43	0.08	0.33
Fr_{5-95}	0.05	0.29	0.32	0.41	0.06	0.73	0.82	1.08	0.41	0.53	0.37	0.13	0.63
Avail. area (m^2)	374	1542	1072	1557	3215	529	3537	195	395	6981	3114	797	1335
% avail. area	1.5	9.3	4.0	5.8	12.8	2.1	14.1	0.8	1.6	27.9	12.7	3.3	5.5
Redds (n)	0	0	0	46	31	14	94	7	19	209	0	0	14
% redds	0	0	0	10.6	7.1	3.2	21.7	1.6	4.4	48.2	0	0	3.2
Redds/m^2	0	0	0	0.032	0.010	0.027	0.027	0.037	0.049	0.030	0	0	0.011
MUSI	−1	−1	−1	0.28	−0.26	0.23	0.23	0.37	0.29	0.49	−1	−1	−0.28
Sediment class	Gravel/ cobble	Cobble/ sand	Boulder/ cobble	Gravel/ cobble	Gravel/ cobble	Gravel/ cobble–boulder/ cobble	Gravel/ cobble–cobble/ gravel	Gravel/ cobble–cobble/ gravel	Gravel/ cobble	Gravel/ cobble	Cobble/ boulder	Gravel/ cobble	Cobble/ gravel/ boulder
Pebble counts (n)	9	6	0	7	0	0	0	0	6	3	10	0	0
d_{50} (mm) mean, range	64.2, 59.7–71.5	74.1, 59.3–92.2	n/a	66.2, 57.3–74.0	n/a	n/a	n/a	n/a	60.9, 53.4–68.1	43.0, 32.2–52.7	83.2, 72.5–97.7	n/a	n/a
d_{90} (mm) mean, range	117.9, 90.6–157.6	178.7, 139.1–212.3	n/a	120.8, 91.8–157.6	n/a	n/a	n/a	n/a	102.9, 88.0–113.0	106.0, 63.1–152.2	165.4, 144.0–199.5	n/a	n/a

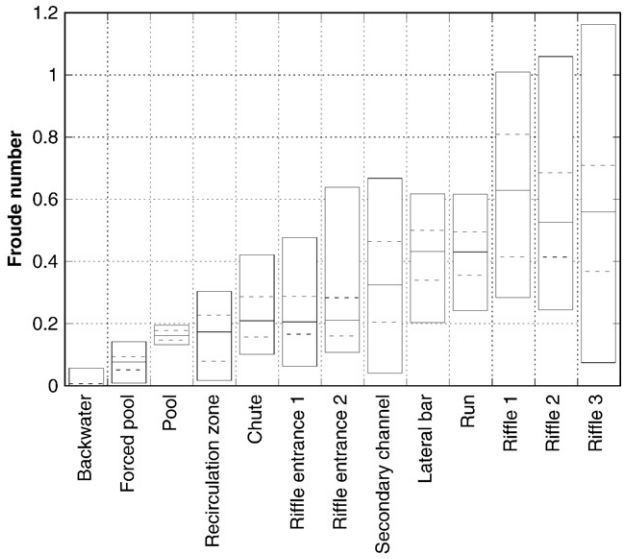

Fig. 8. Percentile plots of model-derived Froude number distributions for individual morphological units. The central line within the box represents the median value of the distribution, the top and bottom of the box are the 5th and 95th percentiles, respectively. Internal dashed lines are the upper and lower quartiles (i.e., 25th and 75th percentiles).

with the second highest proportion of predicted points was adjacent to the actual unit in terms of their geographical distributions (Fig. 2). Although 60.4% of its points were correctly classified, the secondary channel accounts for a substantial proportion of the error in classification in other units (e.g., 27.9% in the recirculation zone). When data from this unit was taken out of the analysis, the proportion of correctly predicted points increased in all units (the mean prediction across all units improved from 57.8% to 67.1%).

4.4. Sedimentary character of morphological units

The qualitative assessment of sedimentary characteristics across the study site showed that the majority of morphological units (9 out of 13) had gravel as the dominant size class (Table 2). The recirculation zone, chute, run and secondary channel had coarser dominant size classes (boulder for chute, the remainder cobble).

As discussed in Section 3.1.4, pebble counts were not carried out at all morphological units due to unwadeable conditions (i.e., too deep and/or fast flowing water). However, the units for which data was obtained show agreement between the qualitative and quantitative assessments; the average d_{50} and d_{90} values of units classified as gravel-dominated (i.e., backwater, lateral bar, and riffle entrances 1 and 2) is 61.3 and 114.6 mm, respectively, compared to 79.8 and 170.4 mm, respectively, for cobble-dominated units (i.e., recirculation zone, run). Of the gravel-dominated units, only the backwater was not 'preferred' (i.e., MUSI > 0) by spawning fish.

4.5. Morphological units and Chinook salmon spawning activity

The locations of redds surveyed in the 2004 season indicate that spawning was concentrated at predictable points (Fig. 7A–C). Spawning tended to occur in locations exhibiting relatively low depth (Fig. 7A), moderate velocity (Fig. 7B) and low to moderate Froude number (Fig. 7C). However, there were also locations meeting these general hydraulic criteria that were not utilized by fish due to unsuitable substrate sizes in those locations (e.g., cobble-dominated material at the channel margin adjacent to the south bank, downstream of the island).

In terms of morphological units, spawning was concentrated at lateral bar, riffle, and riffle entrance locations with sporadic incidents also located in the secondary channel and pool. Raw spawning frequency data reveal that riffle entrance units were the most utilized followed by riffle, lateral bar, pool, and then secondary channel (Table 2). This pattern remained much the same when spawning in morphological units was standardized by area. Only six morphological units had MUSI values > 0 (i.e., "preferred"), these being riffle entrances 1 and 2, riffles 1–3, and the lateral bar. Pool and secondary channel units had MUSI values between −1 and 0 (i.e., "tolerated") while backwater, recirculation zone, chute, run, and forced pool units had no observed spawning/redds and therefore MUSI values of −1 (i.e., "avoided").

The riffle entrance, lateral bar, and riffle units that were preferred by spawners were relatively variable in terms of Froude

Table 3
Results of Kolmogorov–Smirnov test comparing Froude number distribution data for each combination of morphological unit pairs

Unit type	Recirculation zone	Chute	Lateral bar	Pool	Riffle 1	Riffle 2	Riffle 3	Riffle entrance 1	Riffle entrance 2	Run	Forced pool	Secondary channel
Backwater	17.91	24.26	24.68	26.74	22.30	26.98	20.51	21.94	27.10	26.75	**5.29**	24.53
Recirculation zone		8.02	11.34	24.66	9.20	12.92	8.03	**6.02**	10.38	13.90	20.16	20.86
Chute			12.40	24.24	10.89	15.84	8.98	**1.70**	**2.61**	15.16	30.94	14.44
Lateral bar				*36.41*	6.66	**5.25**	6.91	8.63	13.40	**2.01**	30.70	12.45
Pool					29.78	*47.61*	27.65	20.64	*34.60*	*45.30*	*37.53*	*38.85*
Riffle 1						**6.15**	**4.72**	10.06	11.15	7.94	24.60	16.75
Riffle 2							**3.07**	13.47	19.74	8.50	*39.68*	24.20
Riffle 3								8.34	10.85	8.21	22.07	13.85
Riffle entrance 1									**3.58**	12.98	25.29	11.28
Riffle entrance 2										18.28	*42.69*	20.49
Run											*38.08*	19.43
Forced pool												*41.32*

Entries are the Kolmogorov–Smirnov test statistic (XD); those in bold are less than the 90th percentile of XD values (i.e., most similar Froude number distributions), entries in italics are greater than the 10th percentile of XD values (i.e., least similar Froude number distributions).

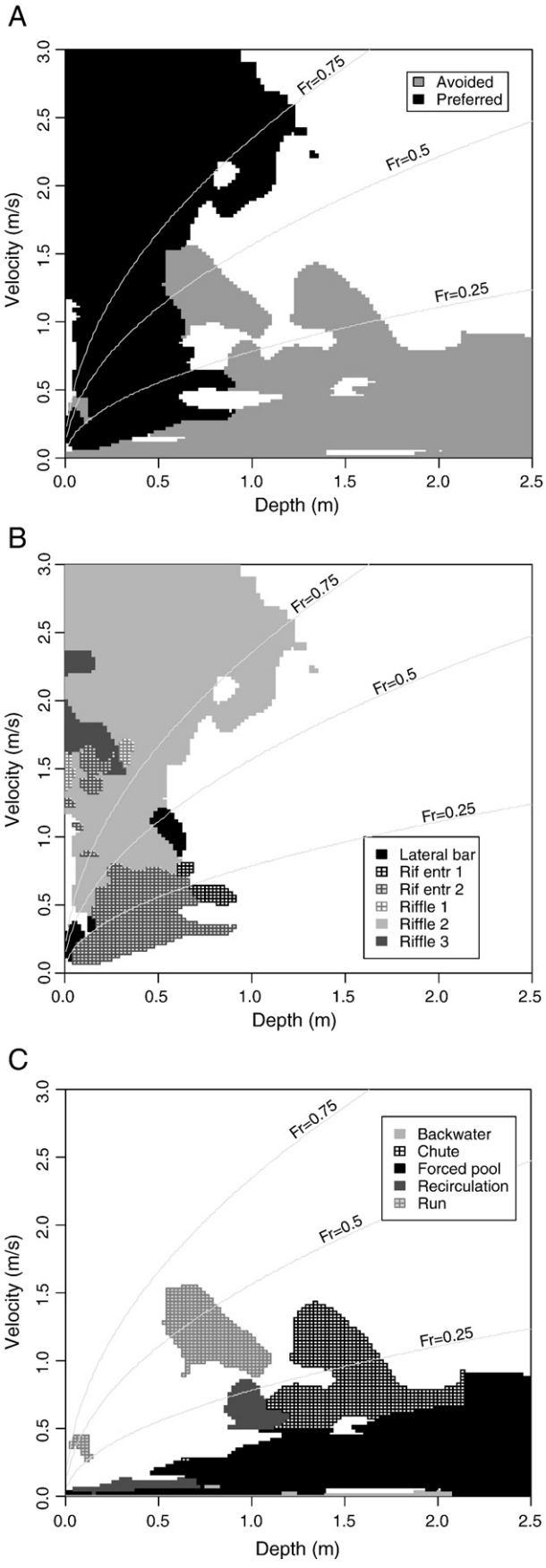

number characteristics (Figs. 7C, 8 and 9B, Table 2); Fr_{50} values range from 0.22 (riffle entrance 1) to 0.63 (riffle 1) and Fr_{5-95} values from 0.41 (lateral bar) to 1.08 (riffle 3). Velocity characteristics (Figs. 7B and 9B) also covered a relatively large range (i.e., U_{50}=0.46 m s^{-1} at riffle entrance 2 to 1.32 m s^{-1} at riffle 3), therefore explaining the relatively wide Froude number range. However, in contrast to their divergent Froude numbers and velocities, median depths were all similarly low for the preferred units (Figs. 7A and 9B, Table 2). The only non-preferred morphological unit to also have a median depth <0.6 m is the backwater class. In summary, all units with MUSI>0 exclusively had H_{50}<0.60 m and U_{50}>0.45 m s^{-1}. In correspondence with these findings, median depth showed the strongest relationship with MUSI among all the morphological units (H_{50}: R^2=0.444, P=0.013; U_{50}: R^2=0.192, P=0.134; Fr_{50}: R^2=0.336, P=0.038).

A higher resolution plot of the hydraulic characteristics of the three types of unit 'preferred' by spawning fish (i.e., riffle, riffle entrance, and lateral bar) is shown in Fig. 10. Given the within-unit hydraulic similarity amongst the three riffles and two riffle entrances apparent in Figs. 7–9 and from the K–S statistic (Table 3), the data from each unit type are combined in Fig. 10. Although there is considerable scatter associated with all three units, a general trend of increasing velocity with depth is evident for the riffle and lateral bar classes. However, the riffle entrance unit exhibits the opposite general relationship with a pattern of decreasing velocity with increasing depth.

5. Discussion

Spawning site characteristics and their spatial distributions are controlled by processes operating at multiple scales (Beechie et al., in press). The physical characteristics of river systems are organized in a nested hierarchy, with physical processes operating at larger scales influencing those at successively finer resolutions (Frissell et al., 1986), ultimately controlling the microscale distribution of instream habitats. The micro and mesoscales are therefore both equally critical elements within this hierarchy with different geomorphic and ecological processes being relevant at these resolutions. For instance, microscale factors will dictate the specific location that a fish selects to spawn while the spatial distribution of mesoscale features will control the locations within a reach where such conditions will exist. An important aspect of the present study was nesting microscale hydraulic data within the larger and ecologically significant scale of the morphological unit. Understanding the mechanistic linkages between the hierarchically organized scales within a river system is necessary to fully understand ecological processes at the catchment scale.

This study has also extended the understanding of mesoscale habitat utilization by spawning salmonids to a larger river system

Fig. 9. Plots of results of KDA: (A) preferred (i.e., MUSI>1) and avoided (i.e., MUSI<1) unit groups, (B) individual preferred units, (C) individual avoided units. Individual hydraulic domains (of individual units or unit groups) are determined by comparing each model output data point to every other data point, identifying which morphological unit it was most probabilistically associated with.

Table 4
Summary of the results of the KDA showing the percentages of data points predicted in each unit type compared to the actual unit type they occurred in (based on field and DEM delineation of the morphological units)

Unit type	Backwater (predicted)	Chute (predicted)	Forced pool (predicted)	Lateral bar (predicted)	Pool (predicted)	Recirculation zone (predicted)	Riffle entrance 1 (predicted)	Riffle entrance 2 (predicted)	Riffle 1 (predicted)	Riffle 2 (predicted)	Riffle 3 (predicted)	Run (predicted)	Secondary channel (predicted)
Backwater (actual)	65.8	0.0	2.4	0.0	0.0	1.7	0.0	0.1	0.0	0.0	0.0	0.0	0.1
Chute (actual)	0.9	61.1	2.4	2.0	3.7	8.0	4.8	2.7	0.0	0.6	0.0	3.2	11.5
Forced pool (actual)	20.6	1.7	69.7	0.0	1.7	8.2	4.8	1.6	0.0	0.0	0.0	0.0	0.7
Lateral bar (actual)	0.3	0.0	0.1	36.8	0.0	0.2	1.3	5.0	0.0	9.9	0.0	4.1	0.6
Pool (actual)	0.0	0.0	0.0	0.0	70.4	0.0	0.0	3.0	0.0	0.0	0.0	0.0	0.0
Recirculation zone (actual)	6.7	8.8	6.1	1.7	3.5	39.1	18.1	3.8	0.0	0.5	0.0	0.4	4.2
Riffle entrance 1 (actual)	0.9	0.2	1.3	1.7	3.6	5.0	45.8	5.1	0.0	2.6	0.0	0.1	2.3
Riffle entrance 2 (actual)	1.7	0.0	4.4	3.7	14.0	4.8	2.2	56.9	4.3	12.5	11.9	0.2	0.2
Riffle 1 (actual)	0.0	0.0	0.0	4.7	0.0	0.0	1.3	0.8	26.1	9.2	21.4	2.1	1.6
Riffle 2 (actual;)	0.3	0.0	0.2	18.0	0.2	1.9	4.0	6.9	30.4	39.9	26.2	8.2	8.1
Riffle 3 (actual)	0.3	0.7	0.1	1.7	0.1	2.6	0.0	1.7	17.4	5.4	35.7	2.5	4.0
Run (actual)	0.3	0.0	0.1	18.0	0.0	0.6	1.3	3.9	4.3	6.8	0.0	57.8	6.1
Secondary channel (actual)	2.3	27.5	13.4	11.6	2.7	27.9	16.3	8.5	17.4	12.6	4.8	21.4	60.4

Cells highlighted grey compare like with like morphological units.

than has typically previously been examined. The application of two-dimensional hydrodynamic modeling enabled a high-resolution quantification of the hydraulic characteristics of the different units present at the spatial scale experienced by fish. Most studies that have attempted to assess the hydraulic characteristics of channel units at the mesoscale have been conducted at a relatively low spatial resolution (e.g., Jowett, 1993; Padmore et al., 1998; Emery et al., 2003). In order that mesoscale physical–biotic linkages can be properly assessed, the resolution of hydraulic information needs to more closely represent that which instream species experience (i.e., <1 m).

5.1. Site-scale distribution of morphological units and interactions with general flow patterns

The study site exhibited a highly heterogeneous channel topography, exemplified by the identification of ten discrete morphological unit types within a section ~8 channel widths in length. The longitudinal and lateral sequences of morphological units across the site provided a wide range of hydraulic and sedimentary conditions. Although heterogeneous across the entire site, hydraulic conditions were well ordered by the underlying topography at the modeled immobile bed low flow. Spatial variation in relative bed elevation and channel width as a consequence of the diverse morphology controlled the mutual adjustment of depth and velocity and was responsible for strong patterns of nonuniform flow (e.g., convergence, divergence, and recirculation). These morphology–flow interactions have important implications for the direct provision of suitable microscale hydraulic conditions and for providing sedimentary characteristics within the mesoscale units that support Chinook salmon spawning, discussed in Sections 5.3.

5.2. Hydraulic characteristics of morphological units

There were considerable differences in hydraulic characteristics between morphological unit types. In most cases the Froude number alone is an adequate hydraulic descriptor to differentiate and group morphological unit types. Indeed, the median and 25th–75th percentile range of Froude number of riffles 1, 2, and 3 are similar despite their very different physical dimensions (e.g., riffle 2 is ~3 times wider and transmits ~2.5 times the discharge under modeled conditions than riffle 1). These data suggest that the dimensionless character of the Froude number may permit the quantitative and generic differentiation between and grouping within certain morphological units types across a range of channel magnitudes or stream orders. A number of other studies have demonstrated that the Froude number is the single best hydraulic parameter to differentiate between morphological units/biotopes (e.g., Jowett, 1993; Rowntree and Wadeson, 1996; Padmore et al., 1998). However, certain units exhibiting contrasting morphologies had very similar Froude number characteristics. Whereas the lateral bar and run units could be argued as being part of the same overall unit (the lateral bar being a subunit of the run located at the channel margins), the chute and riffle entrance units are clearly morphologically and spatially discrete. The

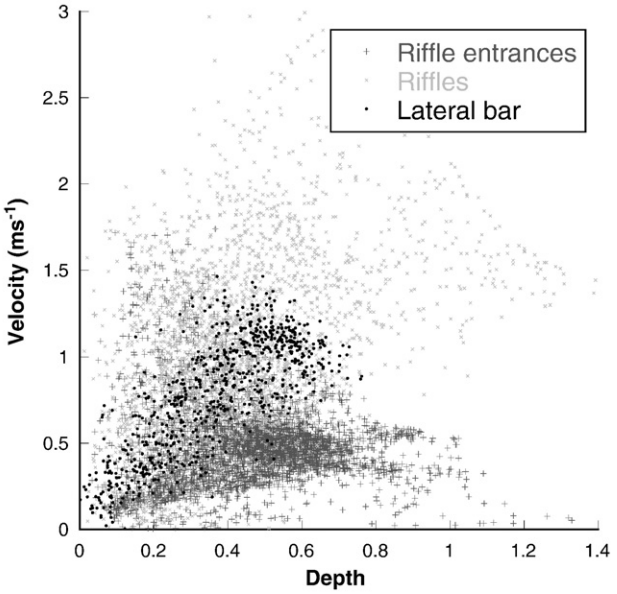

Fig. 10. High-resolution depth–velocity scatter plot for the 'preferred' (i.e., MUSI>1) spawning units (i.e., riffles, riffle entrances, and lateral bar).

chute unit, although having very similar Froude number characteristics, was associated with much deeper flow (and therefore faster mean column velocities) and coarser sediments (from visual assessment) than the riffle entrance units. Therefore, while the dimensionless character of the Froude number may aid in grouping like units in channels of differing magnitude, it also meant that some locations that were very different in terms of geomorphic context and absolute hydraulic characteristics had very similar Froude number values. Moreover, since the sample sizes for each morphological unit are large (ranging between 280 and 3320 data points per unit with a mean of 1,179) the Froude number distributions of all pairings were significantly different (K–S test at $P<0.01$). However, although statistically significant, small differences in the Froude number characteristics between certain units are unlikely to be geomorphically or ecologically significant. For example, the chute and the riffle entrance units are statistically different ($P=0.0084$) but had Fr_{50} values of 0.21 and 0.22, respectively. Therefore, statistical testing with a recognized confidence level was not able to discriminate between Froude number attributes of morphological units. Rather, the 10th and 90th percentiles of the K–S statistic values of test pairings were more useful in identifying the most similar and different morphological units in terms of Froude number. These results showed that, although units with the same classification (i.e., riffles and riffle entrances) were relatively similar to one another, certain unit types that had clearly different physical characters (e.g., chute and riffle entrances) could not be differentiated (i.e., they had relatively low K–S statistic values).

The bivariate plot of the simplified depth–velocity "hydraulic domain" of the "preferred" and "avoided" morphological units (Fig. 9A–C) provided a more detailed insight of the hydraulic functioning at the site. Although not depicting the entire hydraulic scatter across the site, plotting the data in this way offered a compromise between high data resolution and a simplified pattern that aided in identifying the general hydraulic similarities and differences between morphological units exhibiting contrasting levels of spawning utilization. All of the morphological unit types that were identified at the initial survey of the site (and subsequently determined to be "preferred" or "avoided" by spawning Chinook) appeared justified as they were each associated with unique "most probable" locations within the depth–velocity space from the KDA (although, to aid visualization, pool and secondary channel units were not included in the plots). In reality there was considerable overlap in the depth–velocity scatter between morphological units but centers of the distributions were generally discretely located (as identified from the median hydraulic statistics in Table 2). The KDA defined sharp boundaries between morphological units since the procedure predicts the most probable single unit type throughout the available depth–velocity space. This produced discontinuous depth–velocity distributions for certain morphological units; where units overlapped in the depth–velocity space, the unit with the highest density of points in that region was classified as the most probable. In a number of cases (e.g., lateral bar, recirculation zone), this divided a unit type into different regions of the plot. Different morphological units tended to plot in discrete Froude number zones, with riffles being highest and backwater and forced pool lowest (Figs. 8 and 9). However, the depth–velocity plot distinguished between morphological units within the same Froude number zone; riffle entrance, chute, run, and lateral bar units all plotted in discrete locations within the depth–velocity space. Therefore, by plotting hydraulic characteristics on two axes there is a greater ability to differentiate between morphological units.

The KDA results (Fig. 9A–C, Table 4) provided quantitative validation of the morphological unit classifications; in all cases the unit class with the highest proportion of predicted hydraulic data corresponded with the actual unit type as initially identified in the field. However, a large proportion of data points within each unit were misclassified (mean=42.2% including the secondary channel, 32.9% excluding the secondary channel), representing considerable overlap in the depth–velocity scatter between unit types. This is an inevitable situation given that there is a continuum of hydraulics at the site; defining sharp boundaries between morphological units, although necessary for delineation, is at odds with the natural "fuzzy" transition between units. The fact that the KDA results show that the unit type with the second highest proportion of prediction was more likely to be geographically adjacent to the actual unit served to reiterate the influence of "fuzzy" hydraulic boundaries in the segregation of the data.

5.3. Relationships between spawning activity and morphological units

The results of this study demonstrate that Chinook salmon spawning activity was clustered at the mesoscale of specific morphological units. Riffle, riffle entrance, and lateral bar units were found to be "preferred", whereas backwater, recirculation zone, chute, run, and forced pool units were entirely avoided. Although there are inconsistencies in the

definition of morphological units between studies, this finding corresponded with observations made by previous researchers (Geist and Dauble, 1998; Groves and Chandler, 2002; Moir et al., 2002; Hanrahan, 2007). Groves and Chandler (2002) found that most fall Chinook spawning in the Snake River, Idaho occurred in riffles, although this may also incorporate what is defined as riffle entrance in the present study. In the same river system, Hanrahan (2007) found that the upstream and downstream sides of riffles crests (corresponding to riffle entrance and riffle units, respectively, as defined in the present study) accounted for 31% and 53% of Chinook salmon redds, respectively. In the present study, the combined proportion of redds in the equivalent units was similar (79.1%), although individually the fractions were almost exactly reversed (52.6% for riffle entrance and 26.5% for riffle). Some of this difference is likely related to contrasting definitions of morphological units. For instance, Hanrahan (2007) states that 10% of redds occurred in the "downstream end of pools", a region that would likely be incorporated within the riffle entrance in the present study. However, the larger proportion of redds in riffle units reported by Hanrahan (2007) cannot be explained in this way and must be related to other factors (e.g., differing geomorphic controls producing contrasting hydraulic and sedimentary characteristics within riffles; differences in size structure of fish populations, influencing habitat suitability requirements).

In terms of broader scale geomorphic considerations, the highest frequency of spawning utilization at the riffle entrance unit was likely related to the topographic high of the bar/island structure that controls the location of the main riffle crest. The persistence of a riffle at this location is apparent from a sequence of 14 aerial photographs of the study site between 1937 and 2006. Although this topic is the focus of other investigations currently underway, it appears that a valley constriction immediately downstream of the riffle yields a backwater effect during floods that decreases the velocity at the riffle-island location by ~30% when discharge is approximately double bankfull. During low flow, the bar/island feature acts as the hydraulic control for a region of relatively low bed slope, rectangular channel shape and little cross-sectional topographic variation upstream, producing moderate depths and velocities across the entire width of the channel in this area (Stewardson and McMahon, 2002). These hydraulic conditions provide spawning habitat through the direct provision of suitable depth and velocity combinations and by promoting the maintenance of appropriately sized sediments under all but morphology resetting flows.

Although mesoscale Froude number characteristics tend to differentiate between individual morphological unit types and group those given the same classification, they do not discriminate well between those exhibiting contrasting degrees of spawning utilization. The Froude number characteristics of the morphological units "preferred" by spawners covered a relatively wide range. Only at $Fr_{50}<0.2$ do "preferred" morphological units not occur, although the pool unit is "tolerated" ($Fr_{50}=0.16$, MUSI$=-0.27$). Furthermore, there was only a marginally significant relationship between median Froude number and the MUSI value of morphological units ($R^2=0.336$, $P=0.038$). Although salmonid spawning habitat has been shown to be associated with specific Froude number characteristics (Moir et al., 2002), the assessment of this variable at the mesoscale will incorporate locations within a morphological unit that are not suitable (i.e., not all locations within a specific morphological unit will have suitable microhabitat conditions despite that unit being utilized by spawners), thereby reducing the level of explanation. At this spatial resolution, median depth was most closely linked to spawning preference of morphological units by spawning fish ($R^2=0.444$, $P=0.013$ with $R^2=0.192$ and $P=0.134$ for median velocity) and the possible reasons for this are discussed below. The depth–velocity hydraulic domain plot (Fig. 9A–C) better discriminates between morphological units exhibiting different proportional rates of utilization. The bivariate character of the plot allows for the hydraulic differentiation of units that have similar Froude number characteristics but contrasting relative spawning frequencies (i.e., lateral bar and run, riffle entrance, and chute).

The observation that the morphological units associated with the highest relative spawning frequencies occur exclusively in the lower depth region of the hydraulic domain cannot be explained simply in terms of the provision of suitable microscale hydraulic conditions. Although median depths differ between units exhibiting varying rates of relative utilization (i.e., MUSI), there is still sufficient intersection in the depth–velocity space to provide suitable spawning conditions in preferred, tolerated, and certain avoided units (i.e., run and recirculation zone). Two different concepts are proposed to explain the segregation of the "preferred" morphological units to the lower depth region of the hydraulic domain. First, two of the preferred unit types (riffle and riffle entrance) were observed to be hydraulically constricted (both laterally and vertically), and this may provide desirable surface and subsurface hydraulics not captured in the model but recognized and preferred by spawners. Such constrictions provide not only higher surface flow velocities but also stronger velocity gradients. Such gradients may enable spawners to swim over to low-velocity resting habitat quicker and with less effort and have been shown to be especially important in locations lacking cover (Abbe et al., 2002). Previous studies have also reported that flow constrictions force well-oxygenated water into the bed, providing high quality hyporheic conditions for embryo survival that spawners may instinctually recognize (Couloumbe-Pontbriand and Lapointe, 2004). However, no morphological constriction was apparent at the lateral bar unit (also preferred by spawning Chinook) and flow convergence was not as apparent. It is therefore unclear from the results of the present study whether nonuniform flow characteristics are explicitly a condition that spawning Chinook actively select. Nevertheless, the results show that nonuniform flow characteristics as dictated by a heterogeneous channel morphology are important at the mesoscale and the nature of these interactions affect the spatial distribution of suitable microhabitat conditions for spawning Chinook salmon. This distinction between preferred units based on presence/absence of significant nonuniform flow conditions may suggest two discrete types of spawning habitat that are associated with contrasting hydraulic pattern.

Second, characteristic geomorphic conditions (i.e., shear stress/channel competence/transport capacity) at the preferred morphological units promote the maintenance of suitable spawning sediment, a factor not directly accounted for in the hydraulic analysis. Although limited in extent and detail, the sedimentary data in the present study indicate that spawning Chinook select relatively small substrate sizes within the study site (Table 2). This in itself is not a novel finding; it is widely accepted that spawning salmonids select specific substrate sizes (Crisp and Carling, 1989; Kondolf and Wolman, 1993; Moir et al., 2002). Sedimentary factors appear to explain why certain units that provided suitable hydraulic conditions were not utilized by spawning Chinook. The most notable example was the run unit where near ideal combinations of depth and velocity were provided near the channel margins adjacent to the south bank and downstream of the island (Fig. 7). In this location substrate was too coarse for spawning, with cobble-sized material being the dominant size class. The 10 pebble counts conducted within the run unit had mean d_{50} and d_{90} values of 79.8 mm (range = 72.5–97.7 mm) and 165.4 mm (range = 144.0–199.5 mm), respectively, coarser than that quoted as suitable for spawning Chinook salmon (Kondolf and Wolman, 1993). The pertinent question in relation to the present study is therefore not whether spawning Chinook were selecting a certain caliber of sediment (which they clearly did) but, rather, why specific morphological units supported a suitable sedimentary character while others did not?

Large magnitude flood events (i.e., $Q \gg Q_{\text{bankfull}}$) re-set channel morphology and the spatial pattern of sediments, which, in conjunction with river flow, dictate the spatial and temporal distribution of subsequent geomorphic forces. Over time, the mutual adjustment of these factors will result in a quasi-equilibrium state being achieved, with sediments at the site being hydraulically sorted until the next major channel morphology resetting event occurs. The survey of the study site was carried out between April 2004 and April 2005, with the previous large magnitude event ($\sim$3800 m^3 s^{-1}, $\sim$42-yr return interval) occurring on January 1, 1997. Based on aerial photos, a 1999 topographic map from the U.S. Army Corps of Engineers, and field observations, sediments and site morphology appear to have been well adjusted to "normal" geomorphic forces at the time of the study. The only notable site changes 1999 to 2004 were bank erosion on the south side of the island adjacent to the chute and armoring on the main riffle. Spawning habitat can only occur in locations where suitably sized sediment is maintained (i.e., not transported) at flows down to that which spawning occurs (which, in the case of the study site, are the lowest flows in the annual hydrograph). In a large gravel-bed river like the Yuba, the forces acting on the bed near the channel thalweg (where velocity tends to be greatest within a cross-section) are too great even at low flows to permit the maintenance of the mix of gravel and cobble-sized material required by spawning Chinook salmon (Kondolf and Wolman, 1993); thus, areas promoting the preservation of spawning caliber sediment tend to occur in relatively low depth regions of the study site i.e., at channel margins (e.g., lateral bar) and areas with relatively high width:depth ratio (e.g., riffles and riffle entrances). Patterns of shear stress at spawning flows (as could be estimated from the model output) are unlikely to be closely related to mesoscale sedimentary pattern since these are more closely linked to higher flow conditions that are responsible for resetting channel morphology ($Q > 9 \times Q_{\text{bankfull}}$ as observed at the study site). Not all low depth regions are associated with suitable spawning sediment; some locations (e.g., backwater) are also associated with low velocities that promote the deposition of material too fine for spawning (and may also be hydraulically unsuitable for spawning) and, in others, antecedent conditions have provided too high a proportion of large sized material (e.g., recirculation zone). The sedimentary data presented in Table 2 generally support this hydraulic sorting assertion; morphological units with relatively low median depths tend to be associated with smaller sediment sizes.

The high-resolution output from the two-dimensional model identifies that the morphologically-distinct mesoscale units preferentially utilized for spawning (i.e., lateral bar, riffle, and riffle entrance) have distinct hydraulic characteristics (Fig. 10). The riffle entrance locations exhibit a general pattern of decreasing mean column velocity with increasing depth, characteristic of a rectangular channel shape that has little cross-sectional difference in bed elevation but with longitudinal variation in bed slope (Stewardson and McMahon, 2002). Specifically, a downstream topographic high (the riffle crest) acts as a vertical constriction to the flow reducing the cross-sectional area of the channel. Flow continuity dictates that this is associated with an increase in mean velocity, producing a condition of convective acceleration towards the riffle crest and a general pattern of decreasing depth and increasing velocity. The converse pattern of generally co-varying mean column velocity with depth evident for the lateral bar and riffle units indicate a prismatic channel shape with relatively high cross-sectional variation in bed topography but little along the longitudinal axis. In these locations, in the absence of a downstream topographic high, velocity increased with depth towards the channel thalweg as relative roughness and, therefore, flow resistance diminishes. However, despite a similar general depth–velocity trend, important differences in the hydraulic characteristics of riffle and lateral bar units were apparent. The riffle units encompassed a large spatial area and spanned the entire width of the main and secondary channels, producing a broad range of depth–velocity conditions. Also, the tapered constriction of the riffle units produces a convective acceleration effect with velocity increasing in a downstream direction but without an equivalent reduction in the rate of change of depth (as in the riffle entrance units), adding scatter to the plot. The lateral bar unit covered a smaller spatial area and did not extend to the channel thalweg; the associated hydraulic characteristics were therefore over a more restricted range compared to the riffle units. Also, since this unit is not laterally constricted, there is minimal downstream convective acceleration and less scatter in velocity values for a given depth. Furthermore, due to the generally lower energy slope and larger cross-sectional area in the vicinity of the lateral bar unit, velocity tended to be less for a given depth in lateral bar than riffle units.

There was limited opportunity to test whether hydraulic characteristics were consistent by morphological unit type in the present study due to insufficient replication (for the practical

reasons described in Section 3.1.2). Only two unit types had replicates (three riffles and two riffle entrances) and, although these exhibited similar dimensionless hydraulic characteristics (median and range of Froude number; general depth–velocity trends), it is not reasonable to extend this assumption to all unit types. However, since hydraulic patterns are governed by channel geometry and universal river mechanics theory (Stewardson and McMahon, 2002), it is likely that similar types of morphological units as those identified in this study (using the classification described in Section 3.1.2) would at least display the same general trend in joint depth–velocity distribution and approximately equivalent Froude number characteristics, even given differences in stream size. Furthermore, the general character of the unit-specific hydraulic relationships (although not absolute hydraulic parameter values) are likely to be relatively consistent with increasing discharge until a significant channel geometry threshold is breached. This is likely to occur initially at bankfull stage where there is typically an abrupt change in channel cross-sectional shape in alluvial channels as lateral gradient sharply decreases.

Employing an "at-a-station" hydraulic geometry-type approach, Moir et al. (2006) showed that the character of discharge versus depth and velocity relationships were statistically different in mesoscale units of contrasting morphology utilized by spawning Atlantic salmon. Therefore, varying discharge is also likely to be met with contrasting absolute hydraulic responses between different types of preferred morphological units identified in this study. Units that exhibit rapid hydraulic change will show relatively large variation in quantity and/or spatial distribution of habitat availability as flow varies. Other units with more stable hydraulics will provide a more consistent quantity and spatial distribution of suitable habitat over a relatively wide flow range. Webb et al. (2001) demonstrated how individual sites on the Girnock Burn, Scotland were utilized by spawning Atlantic salmon over very specific discharge ranges in three consecutive years (despite contrasting availability of discharge) and speculated that the interaction of discharge with the particular morphology of a site controlled this. These and the findings of the present study suggest that the cumulative effect of a diverse assemblage of morphological units within a section of river will be to provide suitable spawning habitat (and, indeed, habitat for all species and life stages present) over a range of flows; morphological heterogeneity can therefore be regarded as a natural mechanism by which habitat availability can be maintained under a variable discharge regime.

6. Conclusion

The study showed that different morphological units exhibited contrasting characteristics that together provided highly variable conditions across the site for the modeled flow. Despite presumably constant microscale habitat requirements, spawning Chinook salmon preferentially selected specific mesoscale morphological units (lateral bar, riffles, and riffle entrances) that were shown to exhibit opposing depth–velocity relationships (i.e., positive relationship for riffles and lateral bar and negative for riffle entrance) that were controlled by generic nonuniform components of channel geometry. However, all preferred spawning units were shown to display relatively low depth characteristics within that available between all units. In addition to providing appropriate microscale hydraulics, this was thought related to the provision of suitable sedimentary conditions that were hypothesized to be linked to higher flow geomorphic conditions specific to the morphology of these units. Plotting the joint depth–velocity distribution provided the greatest degree of differentiation between unit types although, in most cases, Froude number characteristics alone gave adequate segregation. However, consideration of the joint depth–velocity distribution is essential to capture the specific nature of the relationships between these variables, something the Froude number can only crudely accomplish.

Classic studies by Richards (1976a,b, 1978) demonstrated that riffle and pool units commonly have different channel widths and that variable channel geometry is an implicit condition in gravel-bed rivers. More recent studies have shown that such variations drive nonuniform hydraulics (e.g., convective acceleration, turbulent eddies) that are important to a more complete understanding fluvial and, therefore, ecological processes (Crowder and Diplas, 2006; MacWilliams et al., 2006). The benefits of employing a two-dimensional hydrodynamic modeling approach to resolve mesoscale hydraulics in relation to specific morphological characteristics was demonstrated in this study. The ability of the two-dimensional model to continuously predict hydraulic conditions across the study at the resolution (~1 m) that fish experience them is a clear benefit (Elkins et al., 2007). Also, the resolution of the secondary (lateral) components of stream flow is essential to characterizing convective acceleration, shear zones, and turbulent structures. Such processes play a key role in morphology–flow–sedimentary–hydraulic interactions and are important agents dictating geomorphic character in dynamic gravel-bed systems. Therefore, characterizing these types of channel at the mesoscale using conventional cross-sectional and analytical or pseudo one-dimensional approaches (such as those used in PHABSIM) will fail to capture these nonuniform physical processes that contribute to providing the template for instream habitats.

Restoration of spawning habitat often involves the design of a uniform channel providing suitable microhabitat conditions over a particular range of discharges. This does not explicitly consider morphological complexity, a factor that this study has shown to be closely linked to Chinook salmon spawning habitat and nonuniform geomorphic processes (e.g., convective acceleration) that may be important direct components of habitat and mechanisms for maintaining a quasi-stable channel morphology. This study has shown that a range of unit types promote morphological and hydraulic complexity and it is suggested that this condition provides the template for temporal and spatial habitat dynamics that support suitable microscale conditions for a variety of species and life stages over a range of flows.

Acknowledgements

Financial support for this work was provided by the U.S. Fish and Wildlife Service Anadromous Fish Restoration Program

(Agreement #113323J011). The authors gratefully acknowledge Carlos Alvarado, Blake Andrews, Mary Berta, Mike Bezemek, Evan Buckland, Eve Elkins, Marisa Escobar, Kari Fish, Dave Van Herrick, Lauren Hilliard, Ryan Keating, Cameron Poya, April Sawyer, Carrie Simms, Nakul Thomas, Ben Torchia, Julie Tuck, Conner Voss, and Jason White for their assistance in collection of field data and laboratory analysis.

References

Abbe, T.B., Pess, G.R., Montgomery, D.R., Fetherston, K., 2002. Integrating engineered log jam technology into reach-scale river restoration. In: Montgomery, D.R., Bolton, S., Booth, D.B. (Eds.), Restoration of Puget Sound Rivers. University of Washington Press, Seattle, WA, pp. 443–482.

Acarlar, M.S., Smith, C.R., 1987. A study of hairpin vortices in a laminar boundary layer: Part 1. Hairpin vortices generated by a hemispherical protuberance. Journal of Fluid Mechanics 175, 1–41.

Bates, P.D., Anderson, M.G., Baird, L., Walling, D.E., Simm, D., 1992. Modelling floodplain flow with a two dimensional finite element scheme. Earth Surface Processes and Landforms 17, 575–588.

Bates, P.D., Anderson, M.G., Hervouet, J.M., Hawkes, J.C., 1997. Investigating the behaviour of two-dimensional finite element models of compound channel flow. Earth Surface Processes and Landforms 22 (1), 3–17.

Bates, P.D., Horritt, M.S., Hervouet, J.M., 1998. Investigating two-dimensional, finite element predictions of floodplain inundation using fractal generated topography. Hydrological Processes 12, 1257–1277.

Beechie, T.J., Collins, B.D., Pess, G.R., 2001. Holocene and recent geomorphic processes, land-use and fish habitat in two Puget Sound watersheds. In: Dorava, J.M., Montgomery, D.R., Palcsak, B., Fitzpatrick, F. (Eds.), Geomorphic Processes and River Habitat. American Geophysical Union, Washington D.C., pp. 37–54.

Beechie, T.J., Pess, G., Beamer, E., Lucchetti, G., 2003. Role of watershed assessments in recovery planning for salmon. In: Montgomery, D.R., Bolton, S., Booth, D.B., Wall, L. (Eds.), Restoration of Puget Sound Rivers. University of Washington Press, Seattle, WA, pp. 194–225.

Beechie, T., Moir, H., Pess, G., in press. Hierarchical physical controls on salmonid spawning location and timing. In: DeVries, P., Sear, D. (Eds.), Salmon spawning habitat in rivers: physical controls, biological responses, and approaches to remediation. American Fisheries Society, Bethesda, MD.

Beland, K.F., Jordan, R.M., Meister, A.L., 1982. Water depth and velocity preferences of spawning Atlantic salmon in Maine rivers. North American Journal of Fisheries Management 2, 11–13.

Bovee, K.D., 1986. Development and evaluation of habitat suitability criteria for use in the instream flow incremental methodology. Instream Flow Information Paper 21, U. S. Fish and Wildlife Service Biological Report 86(7), U. S. Fish and Wildlife Service.

Brasington, J., Rumsby, B.T., McVey, R.A., 2000. Monitoring and modelling morphological change in a braided gravel-bed river using high resolution GPS-based survey. Earth Surface Processes and Landforms 25, 973–990.

Brierly, G.J., Fryirs, K., 2000. River styles, a geomorphic approach to catchment characterization: implications for river rehabilitation in Bega catchment, New South Wales, Australia. Environmental Management 25, 661–679.

Brown, L.R., 2000. Fish communities and their associations with environmental variables, lower San Joaquin River drainage, California. Environmental Biology of Fishes 57, 251–269.

Brown, R.A., Pasternack, G.B., in press. Engineered channel controls limiting spawning habitat rehabilitation success on regulated gravel-bed rivers. Geomorphology. doi:10.1016/j.geomorph.2007.09.012.

Buffin-Belanger, T., Roy, A.G., 1998. Effects of a pebble cluster on the turbulent structure of a depth-limited flow in a gravel-bed river. Geomorphology 25, 249–267.

Burner, C.J., 1951. Characteristics of spawning nests of Columbia River salmon. U.S. Fish and Wildlife Service Bulletin 61, 97–110.

Cao, Z., Carling, P., Oakey, R., 2003. Flow reversal over a natural pool-riffle sequence: a computational study. Earth Surface Processes and Landforms 28, 689–705.

Couloumbe-Pontbriand, M.C., Lapointe, M., 2004. Landscape controls on the availability of coarse substrate and winter habitat and their effects on Atlantic salmon (*Salmo salar*) parr abundance patterns along two rivers in the Gaspe Peninsula, Quebec. Canadian Journal of Fisheries and Aquatic Sciences 61, 648–658.

Crisp, D.T., Carling, P.A., 1989. Observations on siting, dimensions and structure of salmonid redds. Journal of Fish Biology 34, 119–134.

Crowder, D.W., Diplas, P., 2002. Vorticity and circulation: Spatial metrics for evaluating flow complexity in stream habitats. Canadian Journal of Fisheries and Aquatic Sciences 59, 633–645.

Crowder, D.W., Diplas, P., 2006. Applying spatial hydraulic principles to quantify stream habitat. Rivers Research and Applications 22, 79–89.

Curtis, J.A., Flint, L.E., Alpers, C.N., Yarnell, S.M., 2005. Conceptual model of sediment processes in the upper Yuba River, Sierra Nevada, CA. Geomorphology 68, 149–166.

Dauble, D.D., Geist, D.R., 2000. Comparisons of mainstem spawning habitats for two populations of fall Chinook salmon in the Columbia River basin. Regulated Rivers 16, 345–361.

Elkins, E.E., Pasternack, G.B., Merz, J.E., 2007. The use of slope creation for rehabilitating incised, regulated, gravel-bed rivers. Water Resources Research 43. doi:10.1029/2006WR005159 W05432.

Emery, J.C., Gurnell, A.M., Clifford, N.J., Petts, G.E., Morrissey, I.P., Soar, P.J., 2003. Classifying the hydraulic performance of riffle-pool bedforms for habitat assessment and river rehabilitation design. River Research and Applications 19, 533–549.

Fischer, H.B., List, E.J., Koh, R.C.Y., Imberger, J., Brooks, N.H., 1979. Mixing in Inland and Coastal Waters. Academic Press, Inc., New York.

Frissell, C.A., Liss, W.J., Warren, C.E., Hurley, M.D., 1986. A hierarchical framework for stream habitat classification: viewing streams in a watershed context. Environmental Management 10, 199–214.

Froehlich, D.C., 1989. Finite Element Surface-Water Modelling Systems: Two-Dimensional Flow in a Horizontal Plane User's Manual. U.S. Department of Transportation, Washington, D.C. Publication #FHWA-RD-88-177.

Fukushima, M., 2001. Salmonid habitat–geomorphology relationships in low gradient streams. Ecology 82, 1238–1246.

Gard, M., 2006. Modeling changes in salmon spawning and rearing habitat associated with river channel restoration. International Journal of River Basin Management 4, 1–11.

Geist, D.R., Dauble, D.D., 1998. Redd site selection and spawning habitat use by fall Chinook salmon: the importance of geomorphic features in large rivers. Environmental Management 22, 655–669.

Grant, G.E., Swanson, F.J., 1995. Morphology and processes of valley floors in mountain streams, Western Cascades, Oregon. Geophysical Monograph 89, 83–101.

Groves, P.A., Chandler, J.A., 2002. The Quality and Availability of Fall Chinook Salmon (*Oncorhynchus tshawytscha*) Spawning and Incubation Habitat Downstream of the Hells Canyon Complex. Idaho Power Company, Boise, ID. Technical Report Appendix E.3.1.3 to FERC Relicensing Application.

Hanrahan, T.P., 2007. Bedform morphology of salmon spawning areas in a large gravel-bed river. Geomorphology 86, 529–536.

Hardy, R.J., Bates, P.D., Anderson, M.G., 1999. The importance of spatial resolution in hydraulic models for floodplain environments. Journal of Hydrology 216, 124–136.

Horritt, M.S., Bates, P.D., Mattinson, M.J., 2006. Effects of mesh resolution and topographic representation in 2D finite volume models of shallow water fluvial flow. Journal of Hydrology 329, 306–314.

Jacobson, R.B., Galat, D.L., 2006. Flow and form in rehabilitation of large-river ecosystems — an example from the Lower Missouri River. Geomorphology 77, 249–269.

James, L.A., 2005. Sediment from hydraulic mining detained by Englebright and small dams in the Yuba basin. Geomorphology 71, 202–226.

Jowett, L.G., 1993. A method of objectively identifying pool, run and riffle habitats from physical measurements. New Zealand Journal of Marine and Fisheries Research 27, 241–248.

Kirkbride, A.D., Ferguson, R.I., 1995. Turbulent flow structure in a gravel-bed river: Markov chain analysis of the fluctuating velocity profile. Earth Surface Processes and Landforms 20, 721–733.

Knapp, R.A., Preisler, H.K., 1999. Is it possible to predict habitat use by spawning salmonids? A test using California golden trout (*Oncorhynchus mykiss aguabonita*). Canadian Journal of Fisheries and Aquatic Science 56, 1576–1584.

Kondolf, G.M., Wolman, M.G., 1993. The sizes of salmonid spawning gravels. Water Resources Research 29, 2275–2285.

Lane, S.N., Richards, K.S., 1998. High resolution, two-dimensional spatial modelling of flow processes in a multi-thread channel. Hydrological Processes 12, 1279–1298.

Lane, S.N., Bradbrook, K.F., Richards, K.S., Biron, P.M., Roy, A.G., 1999. The application of computational fluid dynamics to natural river channels: three-dimensional versus two-dimensional approaches. Geomorphology 29, 1–20.

Lawless, M., Robert, A., 2001a. Scales of boundary resistance in coarse-grained channels: turbulent velocity profiles and implications. Geomorphology 39, 221–238.

Lawless, M., Robert, A., 2001b. Three-dimensional flow structure around small-scale bedforms in a simulated gravel-bed environment. Earth Surface Processes and Landforms 26, 507–522.

Lechowicz, M.J., 1982. The sampling characteristics of electivity indices. Oecologia 52, 22–30.

Leclerc, M., Boudreault, A., Bechara, J.A., Corfa, G., 1995. Two-dimensional hydrodynamic modeling: a neglected tool in the instream flow incremental methodology. Transactions of the American Fisheries Society 124, 645–662.

MacWilliams, M.L., Wheaton, J.M., Pasternack, G.B., Kitandis, P.K., Street, R.L., 2006. The flow convergence-routing hypothesis for pool-riffle maintenance in alluvial rivers. Water Resources Research 42, W10427. doi:10.1029/2005WR004391.

Magee, J.P., McMahon, T.E., Thurow, R.F., 1996. Spatial variation in spawning habitat of cutthroat trout in a sediment-rich stream basin. Transactions of the American Fisheries Society 125, 768–779.

McCuen, R.H., 1989. Hydrologic Analysis and Design. Prentice Hall, Englewood Cliffs, NJ.

Miller, A.J., Cluer, B.L., 1998. Modeling considerations for simulation of flow in bedrock channels. In: Wohl, E.E., Tinkler, K.J. (Eds.), Rivers over Rock: Fluvial Processes in Bedrock Channels. Geophysical Monograph Series. American Geophysical Union, Washington DC, USA, pp. 61–104. #107.

Moir, H.J., Soulsby, C., Youngson, A.F., 2002. Hydraulic and sedimentary controls on the availability and use of Atlantic salmon (*Salmo salar*) spawning habitat in the River Dee system, north-east Scotland. Geomorphology 45, 291–308.

Moir, H.J., Gibbins, C.N., Soulsby, C., Webb, J.H., 2004. Linking channel geomorphic characteristics to spatial patterns of spawning activity and discharge use by Atlantic salmon (*Salmo salar* L.). Geomorphology 60, 21–35.

Moir, H.J., Gibbins, C.N., Soulsby, C., Webb, J.H., 2006. Discharge and hydraulic interactions in contrasting channel morphologies and their influence on site utilization by spawning Atlantic salmon (*Salmo salar*). Canadian Journal of Fisheries and Aquatic Science 2568–2586.

Montgomery, D.R., Buffington, J.M., 1997. Channel reach morphology in mountain drainage basins. Geological Society of America Bulletin 109, 596–611.

Montgomery, D.R., Buffington, J.M., Peterson, N.P., Schuett-Hames, D., Quinn, T.P., 1996. Steam-bed scour, egg burial depths, and the influence of salmonid spawning on bed surface mobility and embryo survival. Canadian Journal of Fisheries and Aquatic Science 53, 1061–1070.

Montgomery, D.R., Beamer, E.M., Pess, G.R., Quinn, T.P., 1999. Channel type and salmonid spawning distribution and abundance. Canadian Journal of Fisheries and Aquatic Science 56, 377–387.

Moyle, P.B., 1994. The decline of anadromous fishes in California. Conservation Biology 8, 869–870.

Newson, M.D., Newson, C.L., 2000. Geomorphology, ecology and river channel habitat: mesoscale approaches to basin-scale challenges. Progress in Physical Geography 24, 195–217.

Nicholas, A.P., Mitchell, C.A., 2003. Numerical simulation of overbank processes in topographically complex floodplain environments. Hydrological Processes 17, 727–746.

Orth, D.J., 1995. Food web influences on fish population responses to instream flow. Bulletin Francais de la Peche et de la Pisciculture 337/338/339, 317–318.

Padmore, C.L., Newson, M.D., Charlton, M.E., 1998. Instream habitat in gravel bed rivers: identification and characterisation of biotopes. In: Klingeman, P.C., Beschta, R.L., Komar, P.D., Bradley, J.B. (Eds.), Gravel Bed Rivers in the Environment. Water Resources Publications, Highlands Ranch, CO, pp. 345–364.

Paola, C., Gust, G., Southard, J.B., 1986. Skin friction behind isolated hemispheres and the formation of obstacle marks. Sedimentology 33, 279–293.

Pasternack, G.B., Wang, C.L., Merz, J.E., 2004. Application of a 2D hydrodynamic model to design of reach-scale spawning gravel replenishment on the Mokelumne River, California. Rivers Research and Applications 20, 205–225.

Pasternack, G.B., Gilbert, A.T., Wheaton, J.M., Buckland, E.M., 2006. Error propagation for velocity and shear stress prediction using 2D models for environmental management. Journal of Hydrology 328, 227–241.

Payne, B.A., Lapointe, M.F., 1997. Channel morphology and lateral stability: effects on distribution of spawning and rearing habitat for Atlantic salmon in a wandering cobble-bed river. Canadian Journal of Fisheries and Aquatic Science 54, 2627–2636.

Rathburn, S.L., Wohl, E.E., 2003. Predicting fine sediment dynamics along a pool-riffle mountain channel. Geomorphology 55, 111–124.

Reeves, G.H., Everest, F.H., Nickelsen, T.E., 1989. Identification of physical habitats limiting the production of coho salmon in western Oregon and Washington. U.S. Forest Service General Technical Report PNW-GTR-245, Boise, ID.

Richards, K.S., 1976a. Channel width and the pool-riffle sequence. Bulletin of the Geological Society of America 87, 877–896.

Richards, K.S., 1976b. The morphology of pool-riffle sequences. Earth Surface Processes and Landforms 1, 87–95.

Richards, K.S., 1978. Channel geometry in the pool-riffle sequence. Geografiska Annaler. Series A 60, 23–27.

Rowntree, K.M., Wadeson, R.A., 1996. Translating channel geomorphology into hydraulic habitat: application of the hydraulic biotope concept to an assessment of discharge related habitat changes. In: Leclerc, M., Boudreault, A., Capra, H., Côté, Y., Valentin, S. (Eds.), Proceedings of the 2nd International Symposium on Habitat Hydraulics, Quebec City. INRS-EAU, Quebec, pp. 342–351.

Shirvell, C.S., 1989. Ability of PHABSIM to predict Chinook salmon spawning habitat. Regulated Rivers Research and Management 3, 277–289.

Stewardson, M.J., McMahon, T.A., 2002. A stochastic model of hydraulic variations within stream channels. Water Resources Research 38, 1–14.

Thompson, J.R., Taylor, M.P., Fryirs, K.A., Brierley, G.J., 2001. A geomorphological framework for river characterization and habitat assessment. Aquatic Conservation: Marine and Freshwater Ecosystems 11, 373–389.

Van Asselt, M.B.A., Rotmans, J., 2002. Uncertainty in integrated assessment modelling — from positivism to pluralism. Climatic Change 54, 75–105.

Vanderploeg, H.A., Scavia, D., 1979. Two electivity indices for feeding with special reference to zooplankton grazing. Journal of the Fisheries Research Board of Canada 36, 362–365.

Webb, J., Moir, H.J., Gibbins, C.N., Soulsby, C., 2001. Flow requirements of spawning Atlantic salmon (*Salmo salar*) in an upland stream: implications for water resources management. Journal of the Institute of Water and Environmental Management 15, 1–8.

Wheaton, J.M., Pasternack, G.B., Merz, J.E., 2004a. Spawning Habitat Rehabilitation-II. Using hypothesis testing and development in design, Mokelumne River, California, U.S.A. International Journal of River Basin Management 2, 21–37.

Wheaton, J.M., Pasternack, G.B., Merz, J.E., 2004b. Use of habitat heterogeneity in salmonid spawning habitat rehabilitation design. In: Garcia, D., Martinez, P.V. (Eds.), Fifth International Symposium on Ecohydraulics: Aquatic Habitats: Analysis and Restoration, IAHR-AIRH: Madrid, Spain, pp. 791–796.

Wolman, M.G., 1954. A method of sampling coarse river-bed material. Transactions of the American Geophysical Union 35, 951–956.